AGU PUBLICATIONS

Geochemistry, Geophysics, Geosystems

RESEARCH ARTICLE
10.1002/2014GC005288

Special Section:
Studies of Seamount Trails: Implications for Geodynamic Mantle Flow Models and the Geochemical Evolution of Primary Hotspots

Louisville Seamount Chain: Petrogenetic processes and geochemical evolution of the mantle source

Loÿc Vanderkluysen[1,2], John J. Mahoney[1], Anthony A. P. Koppers[3,4], Christoph Beier[5], Marcel Regelous[5], Jeffrey S. Gee[3], and Peter F. Lonsdale[3]

[1]School of Ocean and Earth Science and Technology, University of Hawai'i, Honolulu, Hawai'i, USA, [2]School of Earth and Space Exploration, Arizona State University, Tempe, Arizona, USA, [3]Scripps Institution of Oceanography, University of California, San Diego, La Jolla, California, USA, [4]Now at College of Earth, Ocean and Atmospheric Sciences, Oregon State University, Corvallis, Oregon, USA, [5]GeoZentrum Nordbayern, Universität Erlangen-Nürnberg, Erlangen, Germany

Key Points:
- LSC mantle source is surprisingly homogeneous
- A Hawaiian-type tholeiitic shield-volcano stage is absent from LSC seamounts
- LSC mantle source is isotopically distinct from Ontong Java source

Supporting Information:
- ReadMe
- Supplemental Table 1

Correspondence to:
L. Vanderkluysen,
loyc@asu.edu

Citation:
Vanderkluysen, L., J. J. Mahoney, A. A. P. Koppers, C. Beier, M. Regelous, J. S. Gee, and P. F. Lonsdale (2014), Louisville Seamount Chain: Petrogenetic processes and geochemical evolution of the mantle source, *Geochem. Geophys. Geosyst.*, *15*, 2380–2400, doi:10.1002/2014GC005288.

Received 13 FEB 2014
Accepted 16 MAY 2014
Accepted article online 20 MAY 2014
Published online 11 JUN 2014

Abstract The Louisville Seamount Chain is a ~4300 km long chain of submarine volcanoes in the southwestern Pacific that spans an age range comparable to that of the Hawaiian-Emperor chain and is commonly thought to represent a hot spot track. Dredging in 2006 recovered igneous rocks from 33 stations on 22 seamounts covering some 49 Myr of the chain's history. All samples are alkalic, similar to previous dredge and drill samples, providing no evidence for a Hawaiian-type tholeiitic shield-volcano stage. Major and trace element variations appear to be predominantly controlled by small but variable extents of fractional crystallization and by partial melting. Isotopic values define only a narrow range, in agreement with a surprising long-term source homogeneity—relative to the length scale of melting—and overlap with proposed fields for the "C" and "FOZO" mantle end-members. Trace element and isotope geochemistry is uncorrelated with either seamount age or lithospheric thickness at the time of volcanism, except for a small number of lavas from the westernmost Louisville Seamounts built on young (<20 Ma old) oceanic crust. The Louisville hot spot has been postulated to be the source of the ~120 Ma Ontong Java Plateau, but the Louisville isotopic signature cannot have evolved from a source with isotopic ratios like those measured for Ontong Java Plateau basalts. On the other hand, this signature can be correlated with that of samples dredged from the Danger Islands Troughs of the Manihiki Plateau, which has been interpreted as a rifted fragment of the "Greater" Ontong Java Plateau.

1. Introduction

The Louisville Seamount Chain (LSC) is a 4300 km long chain of seamounts and guyots [*Lonsdale*, 1988] in the South Pacific, extending from 139°10′W, 50°26′S, in the vicinity of the Heezen Fracture Zone, to the Tonga-Kermadec Trench (175°18′W, 25°42′S; Figure 1). *Menard et al*. [1964] first reported the existence of an 1100 km long section of the chain. At that time, its origin was linked to the Eltanin fracture zone system, which includes the Heezen and Tharp fracture zones (Figure 1) [*Hayes and Ewing*, 1971; *Larson and Chase*, 1972]. Over the years, however, the hypothesis of a hot spot origin for the Louisville chain has become prevalent [e.g., *Clague and Jarrard*, 1973; *Molnar et al*., 1975; *Jurdy*, 1978; *Lonsdale*, 1988]. Geochronological studies [*Watts et al*., 1988; *Koppers et al*., 2004, 2011, 2012a, 2012b] have shown the existence of an along-chain progression, though not linear, in seamount ages. The oldest dated seamount (78 Ma), Osbourn, is at the northwestern end of the chain; the youngest (1.1 Ma) is in the southeast at 139°9′W. Two first-order bends have been recognized in the chain, at 169°W and 159°W (corresponding to ages of ~47 and 25 Ma, respectively). Long believed to be coeval with a similar bend in the Hawaiian-Emperor chain [e.g., *Lonsdale*, 1988; *Sharp and Clague*, 2002; *Koppers et al*., 2004; *Wessel and Kroenke*, 2009], the 169°W bend is now thought to be older by 3–4 Myr [*Koppers et al*., 2011]. The bend is interpreted as recording changes in Pacific plate motion and/or drift of the Louisville and Hawaiian hot spots.

On the Pacific plate, the LSC is the only other hot spot trail besides the Hawaiian-Emperor chain that covers an age span from ~80 Ma (or more, as several older LSC seamounts are being subducted) [*Timm et al*., 2013] to the Pleistocene. As a result, the LSC is important for testing models based to varying extents on data from the Hawaiian-Emperor chain, such as Pacific plate absolute motion [e.g., *Wessel and Kroenke*, 2008; *Koppers et al*., 2011, 2013; *O'Connor et al*., 2013], the evolution of ocean island volcanism [e.g., *Stearns*, 1966; *Macdonald*, 1968] and the genesis of ocean island basalts (OIB). Previous geochemical studies of the

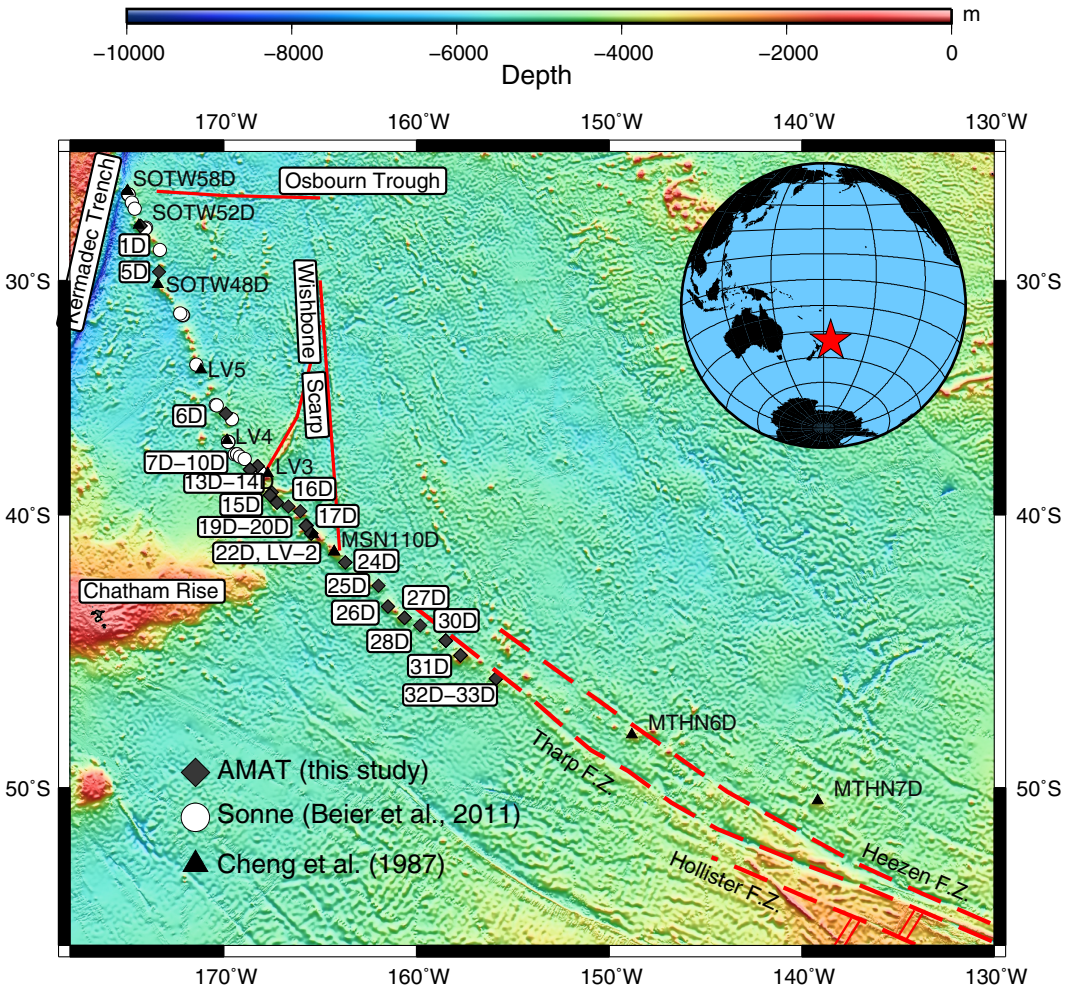

Figure 1. Bathymetric map of the Louisville Seamount Chain (LSC) using GMT [*Wessel and Smith*, 1991, 1998] with existing dredge samples. Inset shows the location of the Louisville Seamount Chain in the South Pacific Ocean. Dredge sites of cruise AMAT02RR for which volcanic samples were recovered are labeled with the dredge number. MSN samples are from the 1961 Monsoon cruise [*Menard et al.*, 1964], SOTW from the 1971 Southtow cruise [*Hawkins*, 1973], LV from the 1979 Vema-36-02 cruise [*Watts et al.*, 1988], and MTHN from the 1984 Marathon cruise [*Lonsdale*, 1988]. F.Z. = fracture zone.

Hawaiian and other ocean islands have documented compositional heterogeneity in the mantle sources [e.g., *Hofmann and White*, 1982; *Staudigel et al.*, 1984; *Rhodes and Hart*, 1995; *Hauri et al.*, 1996; *Sobolev et al.*, 2000]. Such heterogeneity is thought to result from the presence of recycled fragments of lithospheric plates in the earth's mantle, including oceanic crust, lower continental crust, sediments, and/or lithospheric mantle. Such materials are generally envisaged to be in the form of blobs, streaks, or veins within a peridotitic mantle matrix. Moreover, the matrix is itself heterogeneous because of the presence of variably aged residues of variable amounts of partial melting of the mantle, some perhaps dating back to early Earth differentiation [e.g., *Weaver*, 1991; *Hofmann and White*, 1982; *Pilet et al.*, 2005; *Boyet and Carlson*, 2006]. How much of the observed range in isotopic composition of OIB (e.g., in Hawai'i, ε_{Nd} values of Ko'olau shield-stage lavas alone range from −1.9 to +7.3) [*Roden et al.*, 1984, 1994; *Jackson et al.*, 1999; *Salters et al.*, 2006] reflects differences in mantle source composition, as opposed to variations in melting conditions, remains uncertain [e.g., *Keller et al.*, 2000; *Blichert-Toft et al.*, 2003; *Regelous et al.*, 2003; *Ito and Mahoney*, 2005a, 2005b].

One of the factors influencing melting conditions is the seafloor age, and hence the thickness of the lithosphere that is capping the mantle, at the time of emplacement of ocean island volcanoes [e.g., *Haase*, 1996; *Ito and Mahoney*, 2005a]. Louisville volcanoes appear to have formed on oceanic crust of relatively constant age, 40–55 Myr, for much of the chain's history [e.g., *Lonsdale*, 1988]. Exceptions are the westernmost

seamounts of the chain, emplaced on crust that was ≤30 Myr old near the Osbourn Trough, a fossil spreading center [*Lonsdale*, 1988; *Watts et al*., 1988; *Lyons et al*., 2000; *Worthington et al*., 2006]. This situation contrasts with the Hawaiian-Emperor case, where the age of the crust at the time of seamount formation varies considerably. Detroit Seamount, one of the oldest seamounts at the northern end of the chain, was emplaced on very young crust close to a spreading center [e.g., *Cottrell and Tarduno*, 2003], whereas modern Hawaiian volcanoes lie on ~100 Myr old crust [e.g., *Waggoner*, 1993; *Müller et al*., 2008].

The LSC also presents some characteristics that set it apart from other hot spot chains. *Lonsdale* [1988] noted that southeast of the 159°W bend (i.e., seamounts younger than ~25 Ma), average seamount size and therefore volcanic production rates decline sharply; this is coupled with a doubling in average spacing between seamounts. Prior to 25 Ma, magma supply rates appear to have been rather uniform. Evidence from seismic tomography, showing what appears to be a retreating thermal plume [*Montelli et al*., 2004], may indicate that Louisville hot spot activity is waning and that the mantle plume presumed to feed it may be dissipating. Alternatively, *Koppers et al*. [2011] argue that this apparent drop in magma productivity occurred because upwelling from the Louisville plume was partly captured or diverted by a secondary flow toward the Pacific-Antarctic Ridge spreading center.

The LSC lacks any emergent volcanoes and, with a ~2500 km section of the chain located in the latitudes of the "roaring forties," has proven difficult to study. Prior to 2002, chemical analyses existed for only 22 samples dredged from eleven volcanoes [*Hawkins et al*., 1987]. These previously dredged rocks were predominantly alkalic, consisting of alkalic basalts, basanites, trachybasalts, and basaltic trachyandesites with sodic affinity (i.e., hawaiites and mugearites). Age-corrected Sr and Nd isotopic analyses of 15 samples from six seamounts, and eight nonage-corrected Pb isotope analyses, were reported by *Cheng et al*. [1987]. The small range of variation in these data (e.g., age-corrected $\varepsilon_{Nd}(t)$ was between +4.9 and +6.1) led *Cheng et al*. [1987] to suggest that the Louisville mantle source may have remained unusually homogeneous over a period of more than 60 Myr. However, because the rocks were alkalic and came from the upper parts of seamounts, it was unclear whether or not sampling had mainly, or even exclusively, recovered postshield lavas. Indeed, *Hawkins et al*. [1987] speculated that, like Hawaiian volcanoes, the Louisville seamounts might have tholeiitic cores.

In 2002, additional samples were collected during cruise SO167 of the German F.S. Sonne; these rocks too are overwhelmingly alkalic [*Stoffers et al*., 2003; *Beier et al*., 2011]. In 2006, we dredged samples during Leg 02 of the AMAT expedition of the R.V. Revelle, largely from different seamounts than those dredged by the Sonne. Most of the AMAT, and many of the Sonne, dredge hauls were located in scarps and deep incisions on the flanks of volcanoes, in an attempt to avoid postshield flows and access the inferred shield-stage of volcanism in order to determine whether Louisville volcanoes follow the Hawaiian progression of tholeiitic shield and alkalic postshield and rejuvenated stages. Most recently, Expedition 330 of the Integrated Ocean Drilling Program (IODP) drilled into volcanic basement at four LSC seamounts between 26°30′S and 32°13′S [*Koppers et al*., 2012a, 2012b, 2013].

Here we present results of a major and trace element and Sr-Nd-Pb isotopic investigation of lavas dredged during the AMAT expedition from 19 seamounts, including 15 seamounts that had never been previously sampled. The estimated ages of the seamounts range from ~72 to 21 Ma [*Koppers et al*., 2004, 2011]. The aims of the study were to (1) compare the chemical and isotopic differences, if any, between shield and postshield lavas; (2) in combination with *Beier et al*.'s [2011] results, test for any systematic along-chain variations in composition, particularly with respect to the younger, "waning" end of the chain; and (3) assess components involved in the mantle source of Louisville Seamounts. We also evaluate a proposed genetic link between the Louisville hot spot and the Ontong Java Plateau (OJP) [e.g., *Mahoney and Spencer*, 1991; *Richards et al*., 1991; *Tarduno et al*., 1991].

2. Sampling

Thirty-three stations were dredged during AMAT Leg 02, targeting 22 seamounts. At most sites, care was taken to dredge landslide scarps and incisions on the steeper flanks of volcanoes. Eight dredge hauls (2D, 3D, 8D, 9D, 18D, 19D, 21D, and 23D) targeted parasitic cones or summit pinnacles to sample products of the later phases of activity. In all but one case (19D), these eight dredge hauls yielded only sedimentary rocks, foram ooze, corals, and sea stars.

Other dredge hauls recovered ~5–50 cm size volcanic rocks of varied mineralogy, coated with 1–3 mm (and, in rare cases, up to 3 cm) of botryoidal ferromanganese oxide. Dredge 20D, targeting the steep slopes of a gully on a seamount flank, recovered ~50 kg of volcanic rocks from seven visually recognizable lava groups differing in phenocryst assemblage and texture.

The rocks were sawed, split, and described (with the aid of a binocular microscope) on-board. The samples are typically fine-grained and aphyric or olivine and augite-phyric basaltic rocks. The primary mineral assemblage is olivine, clinopyroxene, and plagioclase, with phenocrysts being present in varying amounts and sizes. In the porphyritic samples, phenocryst percentages range up to 30% for olivine, 25% for clinopyroxene, and 10% for plagioclase by volume. Phenocryst sizes range, respectively, from 1–18, 1–11, and 1–3 mm.

Though in many samples the only signs of alteration are ubiquitous ferromanganese coatings and iddingsitization of olivine, visual and microscopic examination reveals, in some, vesicle fillings of carbonate and phosphate (e.g., 6D-3), hydration and devitrification of volcanic glass (e.g., 10D-4), and/or replacement of plagioclase and groundmass phases by clay minerals. Some samples also display a thin palagonite rind, up to 3 mm in thickness.

3. Methods

The least altered, inner cores of samples were selected for analysis. Major element and some trace element concentrations (see supporting information) were determined, respectively, on fused glass disks and pressed powder pellets by X-ray fluorescence (XRF) spectrometry at Washington State University [*Norrish and Chappell*, 1977; *Johnson et al*., 1999]. Powders were prepared by the Washington State University laboratory staff from crushed rock chips using a tungsten carbide mill. Other trace element concentrations (supporting information) were determined by inductively coupled plasma mass spectrometry (ICP-MS) on powders prepared in the same laboratory using a carbon-steel ring mill, following *Knaack et al*. [1994].

Nd and double-spike Pb isotopic ratio determinations and corresponding parent-daughter isotope-dilution measurements (Table 1) were carried out by thermal ionization mass spectrometry at the University of Hawai'i following *Mahoney et al*. [1991, 2005] and *Sheth et al*. [2003]. Isotopic and isotope-dilution analyses were performed on splits prepared from small (1–2 mm) rock chips from the interiors of samples. The chips were picked to avoid alteration and phenocrysts and acid-cleaned in a 0.1 M HF-HNO_3 solution for 5 min prior to dissolution. Concentrations of Pb, Th, U, Nd, and Sm determined by isotope-dilution are generally in good agreement (within $\leq$10%) with the bulk-rock ICP-MS values. The isotope-dilution data are used only for age correction of the isotope ratios because concentrations of small, handpicked, acid-treated chips may not be strictly representative of the whole rocks.

A stronger acid-leaching protocol was adopted for Sr, to remove effects of seawater alteration. About 1 g of whole-rock powder was leached in hot (120°C) 6 M HCl for 6 h in sealed Teflon beakers on a hot plate. The acid was then removed by pipetting, and the leached powder soaked in hot Milli-Q water for an hour. The water was then pipetted off, and the remaining powder washed several times with water, then dried. About 50 mg of the leached powder was digested in HF-HNO_3, evaporated to near dryness, then evaporated several times with 15 M HNO_3 until fully in solution. All reagents used were Teflon distilled. Samples were then dissolved in 2% HNO_3 with trace HF to a dilution factor of approximately 4000. Rb and Sr concentrations were determined using a Thermo X-series 2 quadrupole ICP-MS at the GeoZentrum Nordbayern, Erlangen (Germany). Samples were introduced into the plasma via a Cetac Aridus 2 desolvating membrane unit. Instrument drift was corrected for using a mixed Be-Rh-Bi internal standard, and accuracy and reproducibility were monitored by repeated analyses of the BHVO-2 basalt rock standard. Sr isotopic analyses were carried out on a multicollector ICP-MS at Arizona State University (see Table 1 for analytical details).

4. Results

4.1. Effects of Alteration

Chemically, alteration is expressed in anomalous peaks and/or troughs in Rb, K, U, P, and/or Sr in primitive-mantle-normalized incompatible element patterns (Figure 2a), MnO > 0.25 wt %, and/or elevated weight

AGU Geochemistry, Geophysics, Geosystems

10.1002/2014GC005288

Table 1. Isotopic and Isotope-Dilution Data for Louisville Lavas[a]

Sample	Dredge Site Seamount Name	Dredge Conditions	Estimated Age (Ma)	Distance From Hot Spot (km)	Estimated Age of Crust (Ma)	Age of Crust (Ma) at Time of Loading	Est. Lithosphere Thickness (km)	$^{206}Pb/^{204}Pb_{(0)}$	$^{207}Pb/^{204}Pb_{(0)}$	$^{208}Pb/^{204}Pb_{(0)}$
1D-2	27.6	steep slope, guyot	70	3995	92	22	66	19.339	15.611	39.142
1D-3	27.6	steep slope, guyot	70.8*	3995	92	21.2	65	19.318	15.613	39.280
6D-3	35.8	steep slope, seamount	48	2990	104	56	105	19.101	15.637	39.034
7D-1	168.3	scarp, guyot	50.9*	2670	108	57.1	107	19.606	15.624	39.291
10D-3	*168.6*	*western scarp, guyot*	*49.4**	*2710*	*108*	*58.6*	*107*	*18.914*	*15.622*	*38.916*
13D-1	167.4	scarp, guyot	44	2550	94	50	99	19.348	15.611	39.121
14D-5	167.4	scarp, guyot	44	2550	94	50	99	19.310	15.610	39.090
14D-11	167.4	scarp, guyot	43.9*	2550	94	50.1	99	19.263	15.620	39.136
16D-3	*166.6*	*landslide scarp, guyot*	*43*	*2465*	*92*	*49*	*99*	*19.108*	*15.647*	*38.961*
17D-1	166.1	scarp, guyot	41.3*	2410	91	49.7	99	19.369	15.619	39.153
20D-1	165.7	deep gully, guyot	40	2350	90	50	99	19.364	15.613	39.237
20D-2	165.7	deep gully, guyot	40	2350	90	50	99	19.292	15.608	39.178
20D-3	165.7	deep gully, guyot	39.4*	2350	90	50.6	100	19.593	15.621	39.285
20D-8	165.7	deep gully, guyot	40.4*	2350	90	49.6	99	19.475	15.607	39.231
20D-9	165.7	deep gully, guyot	39.8*	2350	90	50.2	100	19.545	15.623	39.264
22D-4	165.4	flank, guyot	38.9*	2300	89	50.1	100	19.568	15.612	39.242
24D-6	163.6	scarp, guyot	34.7*	2110	84	49.3	99	19.330	15.611	39.087
26D-1	161.5	scarp, guyot	30.3*	1850	77	46.7	96	19.358	15.615	39.159
27D-1	160.7	scarp, guyot	29.3*	1770	76	46.7	96	19.373	15.609	39.126
28D-1	159.8	scarp, seamount	25.6*	1695	73	47.4	97	19.533	15.649	39.055
30D-4	158.5	steep slope, seamount	26	1575	71	45	94	19.507	15.630	39.136
31D-5	157.7	scarp, seamount	24.6*	1490	69	44.4	94	19.341	15.613	39.073
31D-7	157.7	scarp, seamount	24	1490	69	45	94	19.339	15.610	39.076
32D-5	155.9	steep slope, guyot	23	1320	65	42	92	19.253	15.606	39.125
33D-1	155.9	steep slope, guyot	22	1320	65	43	92	19.222	15.593	39.102

Sample	$^{87}Sr/^{86}Sr_{(0)}$(μ)	$^{143}Nd/^{144}Nd_{(0)}$ (μ)	$^{238}U/^{204}Pb$ (μ)	$^{206}Pb/^{204}Pb_{(t)}$ (μ)	$^{207}Pb/^{204}Pb_{(t)}$ (μ)	$^{208}Pb/^{204}Pb_{(t)}$ (μ)	$^{87}Sr/^{86}Sr_{(t)}$ (μ)	ε_{Nd}(t) (μ)	$^{143}Nd/^{144}Nd_{(t)}$ (μ)	Rb/Sr	Pb (ppm)	Nd (ppm)	Sm (ppm)	Th (ppm)	U (ppm)
1D-2	0.70349	0.512880	19.955	19.121	15.600	38.842	0.70344	+5.2	0.512817	0.0170	1.41	26.79	6.091	1.82	0.434
1D-3	0.70364	0.512862	21.997	19.075	15.602	38.747	0.70358	+4.9	0.512800	0.0196	1.10	44.90	10.02	2.49	0.373
6D-3	0.70435	0.512685	15.325	18.986	15.631	38.937	0.70432	+1.3	0.512646	0.0108	5.03	60.12	12.46	3.07	1.19
7D-1	0.70328	0.512869	38.989	19.297	15.610	38.982	0.70327	+4.9	0.512827	0.0015	1.94	43.29	8.971	3.52	1.16
10D-3	*0.70460*	*0.512746*	*43.562*	*18.579*	*15.606*	*38.659*	*0.70386*	*+2.5*	*0.512705*	*0.0092*	*3.14*	*78.49*	*16.33*	*4.95*	*2.13*
13D-1	0.70370	0.512883	36.177	19.100	15.599	38.904	0.70361	+5.1	0.512845	0.0516	2.24	45.20	9.835	3.33	1.25
14D-5	0.70360	0.512878	32.072	19.091	15.599	38.853	0.70360	+5.0	0.512840	0.0038	2.30	46.10	10.10	3.73	1.14
14D-11	0.70356	0.512891	14.913	19.161	15.616	38.918	0.70355	+5.2	0.512852	0.0042	2.39	45.40	10.16	3.57	0.550
16D-3	*0.70382*	*0.512786*	*38.980*	*18.847*	*15.634*	*38.815*	*0.70378*	*+3.2*	*0.512747*	*0.0216*	*1.37*	*33.03*	*7.630*	*1.41*	*0.829*
17D-1	0.70373	0.512902	26.323	19.200	15.611	38.964	0.70369	+5.4	0.512864	0.0231	1.50	37.94	8.870	2.07	0.610
20D-1	0.70402	0.512859	38.101	19.127	15.602	38.989	0.70398	+4.6	0.512825	0.0265	1.81	49.05	10.56	3.36	1.06

Table 1. (continued)

Sample	$^{87}Sr/^{86}Sr_{(t)}$ (μ)	$^{143}Nd/^{144}Nd_{(t)}$ (μ)	$^{238}U/^{204}Pb$ (μ)	$^{206}Pb/^{204}Pb_{(t)}$ (μ)	$^{207}Pb/^{204}Pb_{(t)}$ (μ)	$^{208}Pb/^{204}Pb_{(t)}$ (μ)	$^{87}Sr/^{86}Sr_{(t)}$ (μ)	$\varepsilon_{Nd}(t)$ (μ)	$^{143}Nd/^{144}Nd_{(t)}$ (μ)	Rb/Sr	Pb (ppm)	Nd (ppm)	Sm (ppm)	Th (ppm)	U (ppm)
20D-2	0.70398	0.512844	37.289	19.060	15.597	38.915	0.70393	+4.3	0.512811	0.0280	2.15	54.04	11.42	4.26	1.24
20D-3	0.70346	0.512908	33.919	19.385	15.611	39.065	0.70342	+5.5	0.512873	0.0220	1.70	37.76	8.518	2.85	0.884
20D-8	0.70361	0.512901	43.977	19.198	15.594	38.911	0.70356	+5.4	0.512864	0.0284	1.26	39.09	8.948	2.99	0.851
20D-9	0.70361	0.512907	38.247	19.308	15.612	39.025	0.70357	+5.5	0.512871	0.0261	1.81	44.34	10.11	3.25	1.06
22D-4	0.70347	0.512908	44.809	19.297	15.599	39.014	0.70346	+5.5	0.512874	0.0058	2.21	49.66	10.92	3.88	1.52
24D-6	0.70352	0.512929	16.039	19.244	15.607	38.912	0.70351	+5.9	0.512899	0.0047	2.89	52.06	11.28	4.41	0.715
26D-1	0.70386	0.512901	30.119	19.216	15.608	39.023	0.70381	+5.3	0.512874	0.0333	2.41	42.98	9.756	3.26	1.12
27D-1	0.70351	0.512919	18.022	19.291	15.605	38.956	0.70351	+5.7	0.512893	0.0040	1.80	42.07	9.549	3.15	0.500
28D-1	0.70368	0.512896	66.897	19.266	15.637	38.973	0.70365	+5.2	0.512872	0.0273	2.87	38.70	9.007	2.75	2.95
30D-4	0.70374	0.512915	43.647	19.331	15.622	39.049	0.70372	+5.6	0.512892	0.0232	3.69	53.34	11.95	3.68	2.48
31D-5	0.70377	0.512887	29.910	19.227	15.608	38.960	0.70375	+4.9	0.512862	0.0142	1.51	28.25	7.314	2.11	0.697
31D-7	0.70373	0.512912	33.106	19.215	15.604	38.956	0.70371	+5.5	0.512890	0.0191	1.44	28.13	6.589	2.17	0.735
32D-5	0.70421	0.512834	26.153	19.160	15.602	39.040	0.70418	+4.0	0.512814	0.0308	3.61	45.95	9.927	4.03	1.46
33D-1	0.70417	0.512839	32.499	19.111	15.587	38.981	0.70416	+4.1	0.512820	0.0109	2.00	37.00	8.021	3.31	1.00

[a]All isotopic ratios have been age-corrected (subscript t) to seamount formation age. Italics indicate samples with substantial signs of alteration ("high" or "very high" in supporting information). Ages are interpolated from *Koppers et al.* [2011], with the exception of ages noted with an asterisk (*), which are ^{40}Ar-^{39}Ar ages of *Koppers et al.* [2011]. The hot spot's present location is assumed to be at 50°26.4'S, 139°10'W (the site of sample MTHN-7D) [see *Lonsdale*, 1988]. Present age of the oceanic crust east of the Wishbone Scarp is extrapolated from *Lonsdale* [1988], *Watts et al.* [1988], and *Lyons et al.* [2000]. Estimation of the age of the crust west of the Wishbone Scarp and lithospheric thickness at the time of seamount emplacement is described in the text. Pb and Nd measurements were made on a VG Sector multicollector thermal ionization mass spectrometer at the University of Hawai'i at Mānoa, and Sr analyses were carried out on a Thermo Finnigan Neptune multicollector ICP-MS at the W. M. Keck Foundation Laboratory for Environmental Biogeochemistry at Arizona State University. Data are reported relative to values of $^{87}Sr/^{86}Sr = 0.710238 \pm 0.000018$ (2σ; n = 10) for standard SRM987 Sr, and $^{143}Nd/^{144}Nd = 0.511843 \pm 0.000009$ (n = 28; 0.2 ε_{Nd} units) for La Jolla Nd. Lead isotope ratios were measured with a double-spike method [*Gaderl*, 1999] by dynamic multicollector analysis on 25–50 ng loads of sample. Mean values for 30–40 ng loads of NBS 981 Pb are 16.9406 ± 0.0005, 15.4974 ± 0.0010, and 37.7216 ± 0.0023 for $^{206}Pb/^{204}Pb$, $^{207}Pb/^{204}Pb$, and $^{208}Pb/^{204}Pb$, respectively (2σ, n = 22). Within run errors on the Pb isotopic data are typically 0.002, 0.002, and 0.004 for $^{206}Pb/^{204}Pb$, $^{207}Pb/^{204}Pb$, and $^{208}Pb/^{204}Pb$, respectively. Isotope-dilution concentrations are in ppm. Uncertainties on the isotope-dilution abundances are 0.2% for Sm and Nd, 1% for Pb and U, and 2% for Th. Rb/Sr ratios were measured by ICP-MS. Total procedural blanks were typically ≤25 pg for Pb, <60 pg for Sr, <10 ng for Nd, and ≤2 pg for U and Th. Present-day $\varepsilon_{Nd} = 0$ corresponds to $^{143}Nd/^{144}Nd = 0.512640$; $\varepsilon_{Nd}(t) = 0$ for past times is calculated assuming that $^{147}Sm/^{144}Nd = 0.1967$.

loss on ignition (2.7–11.2 wt %, largely associated with alteration of primary phases to clay minerals but in more highly altered samples also with the presence of carbonate). Less commonly, alteration is also expressed by elevated CaO and Na_2O contents (5D-1 and 30D-3), negative Ce anomalies (e.g., 5D-1, 6D-3, 16D-1, and 24D-2) and, in some samples, high Y relative to Ho and Er (e.g., 5D-1, 6D-3, and 22D-1). Our less altered samples also have a negative Pb anomaly, which is unrelated to alteration, but is instead a common feature of suboceanic mantle melt products [e.g., *Hofmann*, 1988].

For the purpose of this study, we have classified samples using four categories of alteration (supporting information). Samples with "low" degrees of alteration exhibit relatively smooth incompatible element patterns. Patterns of samples with "moderate" alteration display disturbance in the more fluid-mobile elements (Rb, K, U, and Ba) [e.g., *Humphries and Thompson*, 1978; *Seyfried and Bischoff*, 1979], whereas "highly" altered samples also show elevated La/Ta ratios (>14; possibly as a result of marine sediment or ferromanganese infiltration) [e.g., *Hole et al*., 1984], peaks at Sr and P (resulting from precipitates of secondary phosphate and carbonate) and, occasionally, positive Y and negative Ce anomalies (which, together with elevated La and Lu, may result from marine phosphatization). "Very highly" altered samples show all the above characteristics, plus very pronounced enrichments of P and Sr. In the figures used for interpretation of mantle source and petrogenesis, we do not include data for the highly or very highly altered samples.

Some highly and very highly altered samples that we analyzed

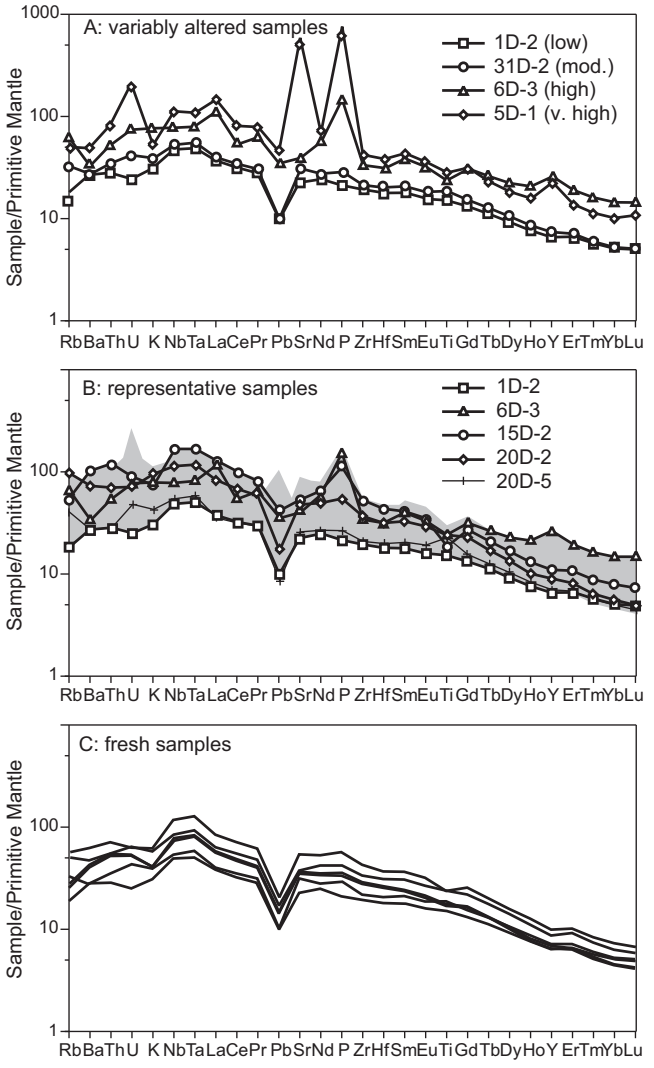

Figure 2. Primitive-mantle-normalized incompatible element patterns of some LSC samples, using normalizing values of *Lyubetskaya and Korenaga* [2007]. (a) Effects of alteration are illustrated by patterns of four variably altered samples. (b) Representative patterns showing the range of observed incompatible element behavior. Patterns of samples 20D-5 and 20D-2 bracket the range of compositions found in the same seamount. Gray field represents the total observed variation among lightly to highly altered samples. (c) Patterns of all samples determined to have undergone low degrees of alteration.

isotopically display variably elevated age-corrected $(^{87}Sr/^{86}Sr)_t$ (0.7038–0.7043 versus 0.7035–0.7039 for the other less altered samples), which can be attributed to seawater-derived alteration not removed during sample preparation. In addition, six samples (6D-3, 10D-3, 14D-11, 16D-3, 28D-1, and 30D-4) have elevated (>15.620) values of age-corrected $(^{207}Pb/^{204}Pb)_t$ and, for three of them, elevated $(^{208}Pb/^{204}Pb)_t$ when compared to their $(^{206}Pb/^{204}Pb)_t$ ratio. This is a common occurrence among highly altered oceanic basalts, as a result of Pb contamination derived from pelagic sediments, ferromanganese, and/or phosphates, which can have Pb concentrations orders of magnitude larger than those of basalts [e.g., *De Carlo et al*., 1987; *Ingram et al*., 1990; *Baturin and Yushina*, 2007]. Three of these six samples, 6D-3, 10D-3, and 16D-3, have the lowest $(^{206}Pb/^{204}Pb)_t$ (<19.0) and $\varepsilon_{Nd}(t)$ (<+4) values. Although Nd isotope ratios are typically much less affected by low to moderate levels of seawater alteration [e.g., *McCulloch et al*., 1981; *Verma*, 1992; *Mahoney et al*., 1998], marine ferromanganese and phosphate phases also have much higher Nd and Sr contents than basalts. Alternatively, *Cheng et al*. [1987] noted that one of their most altered samples had anomalously low ε_{Nd} and attributed it to rare earth element mobility during prolonged low-temperature alteration and/or during palagonitization of basaltic glass. With the exception of 6D-3, 10D-3, and 16D-3, our age-corrected isotopic data define a small overall range of values (see below).

4.2. Major and Trace Elements

Major element analyses (supporting information) indicate that the majority of samples are nepheline-normative alkalic basalts; a few are basanites, and two are trachybasalts (Figure 3a). Our data overlap noticeably with those of *Hawkins et al*. [1987] and *Beier et al*. [2011], and with shipboard data for IODP Expedition 330 lavas [*Koppers et al*., 2012a], which drilled four of the seamounts dredged during the AMAT and Sonne cruises. Magnesium number (Mg# = molar $Mg/[Mg+Fe^{2+}]$, assuming 85% of total Fe is Fe^{2+}) varies from 0.22 to 0.68. Major element trends include increases in TiO_2 and Al_2O_3 (Figures 3b and 3c) and a decrease in CaO/Al_2O_3 (Figure 3d) as Mg# decreases. Despite variable amounts of alteration, Na_2O and K_2O also increase broadly with decreasing Mg#, whereas CaO and FeO exhibit no systematic behavior. Magnesium number is

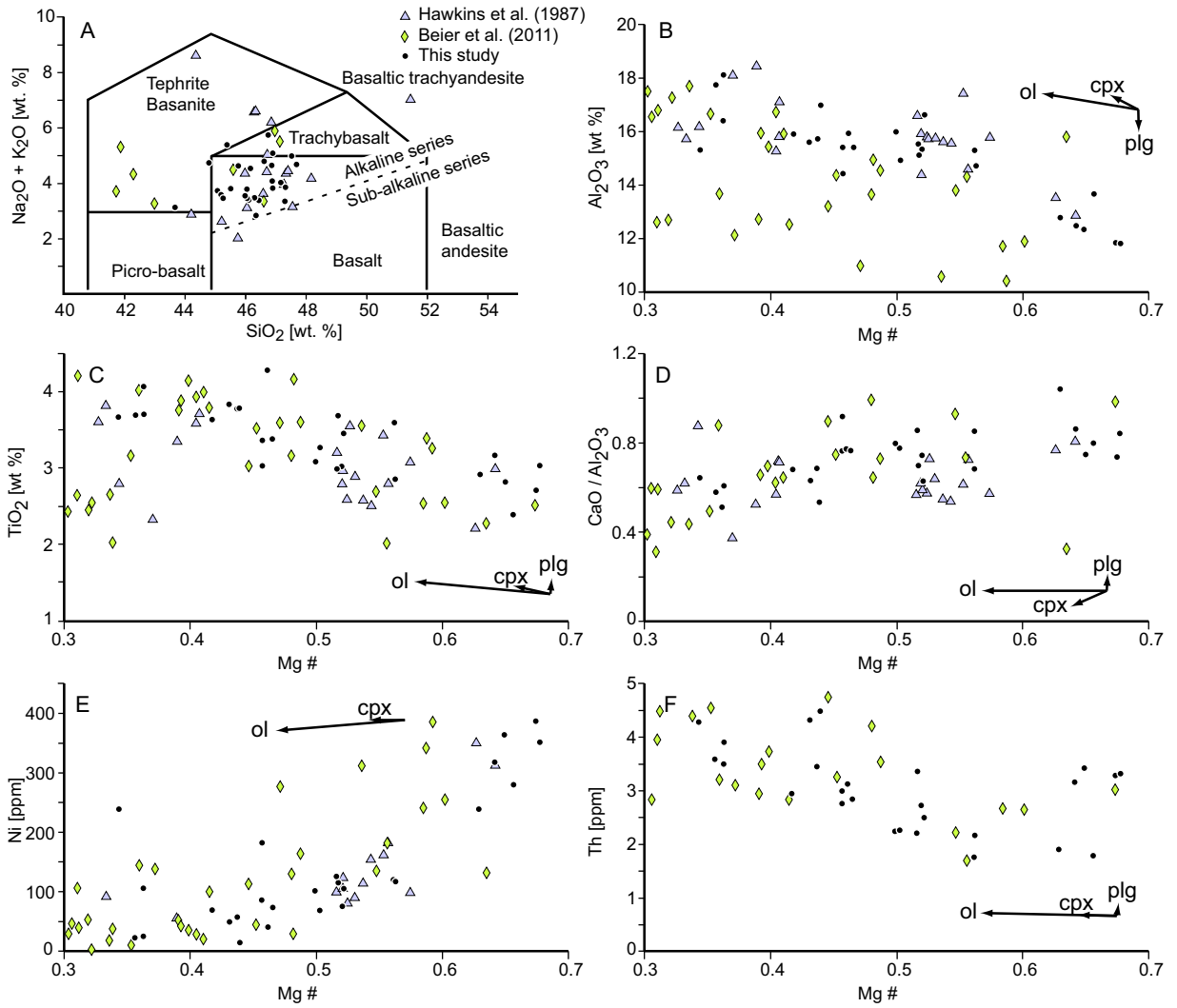

Figure 3. (a) Total alkalis versus silica [*Le Bas et al.*, 1986] classification diagram. Dashed dividing line between alkaline and subalkaline rocks is after *Macdonald and Katsura* [1964]. (b) Al_2O_3, (c) TiO_2, (d) CaO/Al_2O_3, (e) Ni, and (f) Th variation with Mg# in LSC lavas. Samples with "high" and "very high" degrees of alteration are omitted from all panels. Arrows represent the fractionation vectors of olivine (ol), clinopyroxene (cpx), and plagioclase (plg), based on published mineral data of LSC samples [*Hawkins et al.*, 1987].

positively correlated with concentrations of compatible trace elements (e.g., Ni and Cr) and negatively correlated with incompatible trace elements (e.g., Th and La) (Figure 3).

Primitive-mantle-normalized incompatible element patterns show variations bounded by three extreme compositions (Figure 2b). One type (e.g., sample 1D-2) is characterized by a relatively flat pattern (mantle-normalized $(Nb/Zr)_N \leq 2.5$ and $(Sm/Lu)_N < 4$) displaying modest overall enrichment of incompatible elements relative to model primitive-mantle values (e.g., Nb < 45, Zr < 19, and Lu < 4.5 times the primitive-mantle estimates of *Lyubetskaya and Korenaga* [2007]). Another type (e.g., 6D-3) has similarly flat patterns, but greater absolute enrichment (e.g., Yb > 9 times primitive-mantle estimates); samples of this type are more evolved, with lower Mg#, and Ni and Cr contents. The third type (e.g., 15D-2 and 20D-2), which broadly corresponds to the more alkali-rich samples, has more steeply sloping patterns overall, $(Sm/Lu)_N > 5.5$ and $(Nb/Zr)_N > 2.6$. Interestingly, nearly the full range of pattern slopes and levels of incompatible trace element enrichment is observed in a single seamount (samples 20D-2 and 20D-5 have $(Sm/Lu)_N = 6.6$ and 4.2, $(Nb/Zr)_N = 3.0$ and 2.5, and Nb = 52 and 25 ppm, respectively; Figure 2b). Sample 19D-1, which was dredged on a pinnacle likely representing a late-stage of volcanism (and possibly erosional in origin), is indistinguishable from other samples from its major and trace element composition. Moreover, there is no

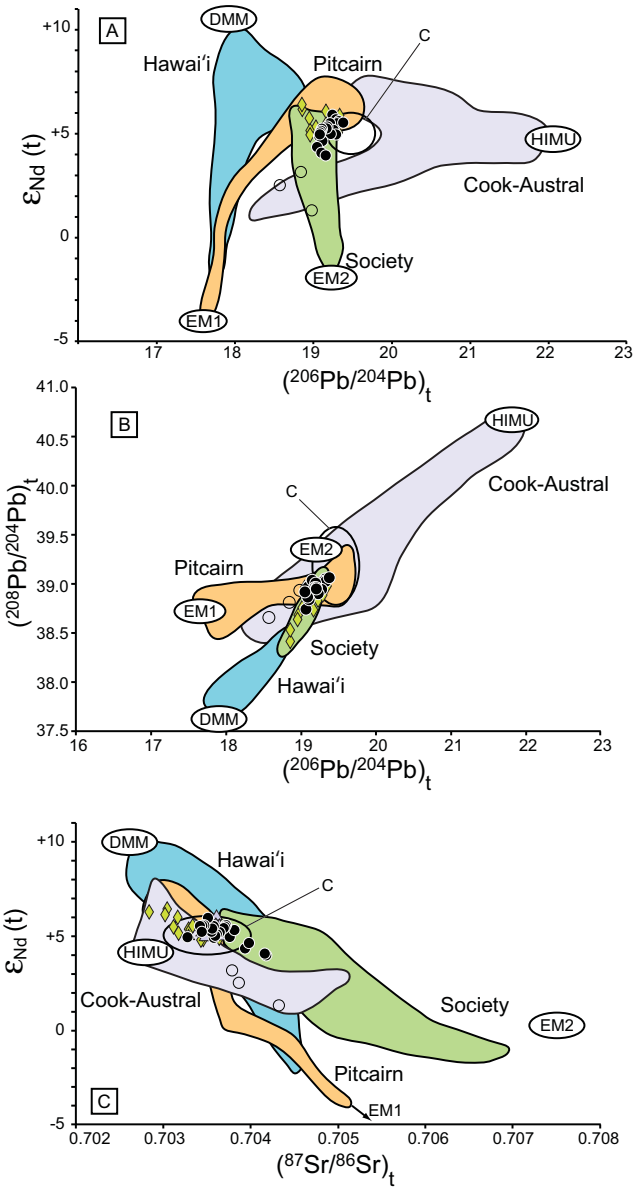

Figure 4. Age-corrected Sr, Nd, and Pb isotopic ratios of Louisville samples. Black dots: this study; green diamonds: *Beier et al.* [2011]; blue triangles: *Cheng et al.* [1987]; open circles: highly altered samples of this study. The colored fields enclose present-day values for four other Pacific hot spot islands or island groups. Pitcairn data are from *Woodhead and McCulloch* [1989], *Dupuy et al.* [1993], and *Cotten et al.* [1995]; Cook-Austral from *Nakamura and Tatsumoto* [1988], *Chauvel et al.* [1997], and *Lassiter et al.* [2003]; and Society from *Devey et al.* [1990], *Cheng et al.* [1993], *Hemond et al.* [1994], and *White and Duncan* [1996]. Hawai'i data are from *Stille et al.* [1983], *Roden et al.* [1984, 1994], *Chen and Frey* [1985], *West and Leeman* [1987], *West et al.* [1987], *Chen et al.* [1990, 1996], *Frey et al.* [1994], *Rhodes and Hart* [1995], *Basu and Faggart* [1996], *Reiners and Nelson* [1998], *Pietruszka and Garcia* [1999], *Abouchami et al.* [2000, 2005], *Regelous et al.* [2003], *Blichert-Toft et al.* [2003], *Eisele et al.* [2003], *Huang et al.* [2005], *Shafer et al.* [2005], *Blichert-Toft and Albarède* [2009], and *Weis et al.* [2011]. Boxes marked DMM, HIMU, EM1, and EM2 indicate the postulated mantle end-member components of *Zindler and Hart* [1986], whereas area "C" is after *Hanan and Graham* [1996].

systematic variation in major or trace element composition with volcano age or seamount location within the chain over most of its length, except for the northwestern-most seamounts, where lavas extend to lower Nb/Zr and La/Yb [*Beier et al.*, 2011].

4.3. Isotopic Composition

Despite the fact that the samples represent a nearly 50 Myr time span of Louisville hot spot volcanism, their age-corrected isotopic ratios define only a narrow range (Figure 4), overlapping substantially with the data of *Cheng et al.* [1987] and, for Nd and Pb, with those of *Beier et al.* [2011]. Excluding the three highly altered samples noted above (open circles in Figure 4), our $\varepsilon_{Nd}(t)$ values range from +4.0 to +5.9, whereas Cheng et al.'s range from +4.9 to +6.1 (after recalculating their values from the reported ε_{JUV} to ε_{Nd}) and *Beier et al.*'s [2011] from +4.8 to +6.5. Variation in the age-corrected values is only 0.325 in $(^{206}Pb/^{204}Pb)_t$ (19.060–19.385) and 0.318 in $(^{208}Pb/^{204}Pb)_t$ (38.747–39.065). *Cheng et al.*'s [1987] Pb isotope data were not age-corrected but cover a range of similar values (19.128–19.452). *Beier et al.*'s [2011] age-corrected Pb isotopic data overlap substantially with ours, although values for five of their samples extend to lower $(^{206}Pb/^{204}Pb)_t$ between 18.972 and 18.865. Our range in $(^{87}Sr/^{86}Sr)_t$ is 0.70327–0.70398 (again excluding five of the more highly altered samples), whereas $(^{87}Sr/^{86}Sr)_t$ values for *Cheng et al.*'s [1987] samples are between 0.70329 and 0.70375. *Beier et al.*'s [2011] $(^{87}Sr/^{86}Sr)_t$ values range from 0.70285 to 0.70365.

No apparent isotopic difference exists between the basalts and basanites or trachybasalts. Nor is there any systematic isotopic variation with indicators of the degree of partial melting (e.g., La/Yb) or fractionation (e.g., Mg#; see Figure 7). For example, the maximum range in $\varepsilon_{Nd}(t)$ is seen in samples with a very small

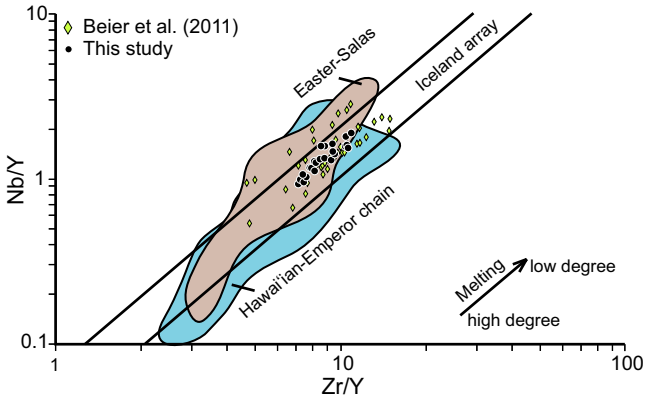

Figure 5. Variation of LSC samples in Nb/Y and Zr/Y, two trace element ratios indicative of the effects of partial melting and source heterogeneity. Array for Iceland is from *Fitton et al.* [1997]. Field for the Hawaiian-Emperor chain is from *Bence et al.* [1980], *Cambon et al.* [1980], *Dalrymple et al.* [1981], *Frey et al.* [1994], *Rhodes and Hart* [1995], *Chen et al.* [1996], *Pietruszka and Garcia* [1999], *Regelous et al.* [2003], *Huang et al.* [2005], and *Shafer et al.* [2005]. Field for Easter-Salas y Gómez hot spot trail is from *Baker et al.* [1974], *Bonatti et al.* [1977], *Puzankov and Robrov* [1997], *Haase et al.* [1997], and *Ray et al.* [2012]. Arrow indicates the effect of varying degrees of partial melting of a single peridotitic source.

range in La/Yb of 17–18. As with incompatible element patterns, the maximum variation observed in $(^{206}Pb/^{204}Pb)_t$ among our samples occurs among five rocks recovered from dredge 20D, which also vary over a significant portion of the measured total range in $\varepsilon_{Nd}(t)$ (from +4.3 to +5.5).

5. Discussion

The behavior of the major elements (Figures 3b–3f) and compatible trace elements in our AMAT data set is consistent with control by fractional crystallization of olivine and clinopyroxene, as also concluded for many other LSC samples by *Hawkins et al.* [1987], *Beier et al.* [2011], and *Koppers et al.* [2012a]. The trends observed in Al_2O_3 and CaO/Al_2O_3 (Figures 3b and 3d) preclude plagioclase from having played a dominant role in the fractionating assemblage. The scatter in major element concentrations at a given Mg# (notably Al_2O_3; Figure 3b), however, points to the presence of a range of parental liquids to LSC lavas, generated in a range of melting conditions. This is consistent with the trace elements behavior (cf. section 5.2). Previous authors have noted some high-MgO LSC rocks (with Mg# >0.65; not shown in Figure 3) that are interpreted as having accumulated olivine [e.g., *Hawkins et al.*, 1987], but our data set lacks such samples.

In a Zr/Y versus Nb/Y diagram (Figure 5) [*Fitton et al.*, 1997], our data define an array parallel to and within that for Icelandic lavas. Although developed specifically to understand lavas from Iceland, such diagram is useful when interpreting all OIB, because Zr and Nb are both incompatible elements, and behave very similarly during melting of mantle rocks compared to the less incompatible element Y. Thus, varying amounts of partial melting of a uniform peridotitic source will produce an array approximately parallel to the Icelandic array. Variability of mantle source composition can be expressed by variations in Nb/Zr at relatively low degrees of partial melting [e.g., *Fitton et al.*, 1997; *Pfänder et al.*, 2007]. Fractional crystallization, on the other hand, will have little or no effect on these ratios as long as the melts are zircon-unsaturated, which is generally the case in basalts [e.g., *Belousova et al.*, 2002; *Hoskin and Schaltegger*, 2003]. Our data array is particularly short and narrow relative to the fields defined by Iceland and many other hot spot-related islands and seamount chains.

Both incompatible element and isotopic ratios suggest that the Louisville mantle source was remarkably homogeneous over much of its history (Figures 4 and 5). The isotopic signature is broadly "C" or "FOZO" type [e.g., *Hart et al.*, 1992; *Hanan and Graham*, 1996; *Stracke et al.*, 2005]. These authors argued that these compositions represent material fed to the upper mantle by deep-sourced mantle plumes. C and FOZO are commonly occurring sources in ocean island basalts and are thought by some workers to be the signatures of mantle that underwent melt depletion early in the Earth's history [e.g., *Hart et al.*, 1992; *Boyet and Carlson*, 2006], or to originate from a highly heterogeneous and well-stirred mixture of recycled oceanic crust [e.g., *Kellogg et al.*, 2004]. The small variation in LSC isotopic ratios is particularly impressive when the results are compared to data for other Pacific hot spots (e.g., Figure 4). For comparison, the total variation in $(^{206}Pb/^{204}Pb)_t$ (0.325) along the LSC over the ~49 Myr of its history covered by our samples is comparable to the variation (0.302) observed at the Kilauea volcano of Hawai'i just since 1917 [*Pietruszka and Garcia*, 1999].

5.1. Lithospheric Thickness at the Time of Volcanism

In a hot spot setting, melting conditions may be constrained by the thickness of the lithosphere at the time of seamount formation (which controls the depth of the top of the melting region). Oceanic lithosphere

thickness is primarily a function of its age [e.g., *Sclater et al*., 1977; *Stein and Stein*, 1992; *Kawakatsu et al*., 2009]. To assess the degree to which the geochemical signatures of LSC seamounts are related to variations in melting conditions, it is thus necessary to estimate crustal age at the time of seamount emplacement. We first estimated the present age of crust beneath each seamount. For the seamounts that we sampled along the younger southeastern part of the chain (our dredge sites 24D–33D; Figure 1), built on crust accreted during magnetic chrons C33r–C28, the age of the crust was provided by the magnetic anomalies identified by *Lonsdale* [1988], *Watts et al*. [1988], and *Lyons et al*. [2000]. The remaining seamounts are on crust accreted during the Cretaceous Long Normal period, thereby lacking identifiable magnetic anomalies. For the sampled seamounts on Cretaceous Magnetic Quiet Zone between site 24D and the western Wishbone Scarp (sites 23D–15D), we extrapolated crustal ages northwestward using the spreading rate recorded by Chron C33. We accept the interpretation of *Lonsdale* [1997], *Worthington et al*. [2006], and *Downey et al*. [2007] that Cretaceous oceanic crust west of the western Wishbone Scarp is the southern flank of a separate "Osbourn Rise" that had the now extinct Osbourn Trough as its spreading axis, and originated by the separation of Hikurangi Plateau from Manihiki Plateau. *Worthington et al*. [2006] argue that this spreading center was active from 120–115 to ~86 Ma, and we use these dates for simple interpolation of isochrons across the southern flank of the rise to derive approximate crustal ages at the seamounts from which samples 1D–14D were collected.

We calculated the age of the crust at the time of seamount emplacement, by subtracting seamount ages, based on the ^{40}Ar-^{39}Ar dates, or interpolated from the data, of *Koppers et al*. [2004, 2011]. For example, we infer that Osbourn Seamount at 25.9°S, the oldest sampled seamount in the chain with a sample age of 78.8 Ma [*Koppers et al*., 2004], was emplaced on ~10 Myr old crust, and that seamount 27.6°S formed on ~20 Myr old crust, somewhat greater than the ~10 Myr estimated by *Contreras-Reyes et al*. [2010] on the basis of a plate elasticity argument (these authors misidentify seamount 27.6°S as Louisville Guyot, which is ~450 km further south). We then calculated lithospheric thickness (Table 1) using a simple half-space cooling model [*Turcotte and Schubert*, 1982] and the assumption that the lithosphere's lower boundary corresponds to the 1200°C isotherm. Though the exact nature of the lithosphere-asthenosphere boundary is likely more complex, this cooling-to-thickness relationship seems to remain broadly applicable for oceanic plates [e.g., *Kawakatsu et al*., 2009; *Rychert and Shearer*, 2009]. The calculated thicknesses range only narrowly from 92 to 107 km, except for the northernmost seamount that we dredged, for which the estimated lithospheric thickness at the time of volcanism is 65–66 km.

5.2. Melting Model

To evaluate the conditions and extent of melting, we employed the REEBOX melting algorithm [*Fram and Lesher*, 1993; *Fram et al*., 1998; *Tegner et al*., 1998]. This approach differs from that of *Hawkins et al*. [1987], who assumed fractional melting of a garnet lherzolite source to account for their Zr/Nb and Zr/Y data. They estimated a range of 5–9% of partial melting. The REEBOX program calculates the trace element composition of pooled melts formed by aggregation of nonmodal incremental melts produced in 0.1 GPa increments over a range of pressures. The melting reactions depend on the mineral assemblage in the source [see *Fram et al*., 1998]. Mantle composition and modal mineral assemblage are revised at each increment to take into account depletion due to melting and pressure-dependent phase transitions, with the garnet-spinel and spinel-plagioclase transitions occurring between 3–2 GPa and 1.4–1 GPa, respectively. The total fraction and composition of melt are a function of the depth at which melting starts (a proxy for mantle temperature) and ends (where mantle upwelling stops). We used mineral-melt partition coefficients from *Salters and Stracke* [2004] and assumed premelting mantle proportions of 0.50:0.25:0.15:0.10 of olivine:orthopyroxene:clinopyroxene:garnet/spinel. The sensitivity of the model primarily depends on the chemical composition of the source and is rather robust to variations in mineral abundances in the source for small to moderate amounts of partial melting. The amount of garnet in the source is, however, relatively well constrained by the modeling, because this mineral strongly influences the heavy rare earth elements (though the exact starting amount depends in part on partition coefficients used). In addition, it should be noted that the premelting mineral proportions in this model do not capture the likely complex mineralogical nature of alkalic OIB mantle sources [e.g., *Hirschmann et al*., 2003; *Dasgupta et al*., 2006, 2007], and results should thus be interpreted qualitatively. We find that starting lithologies with little or no olivine do not adequately reproduce our data. However, this does not in itself rule out the possibility of such lithologies being present in the source region.

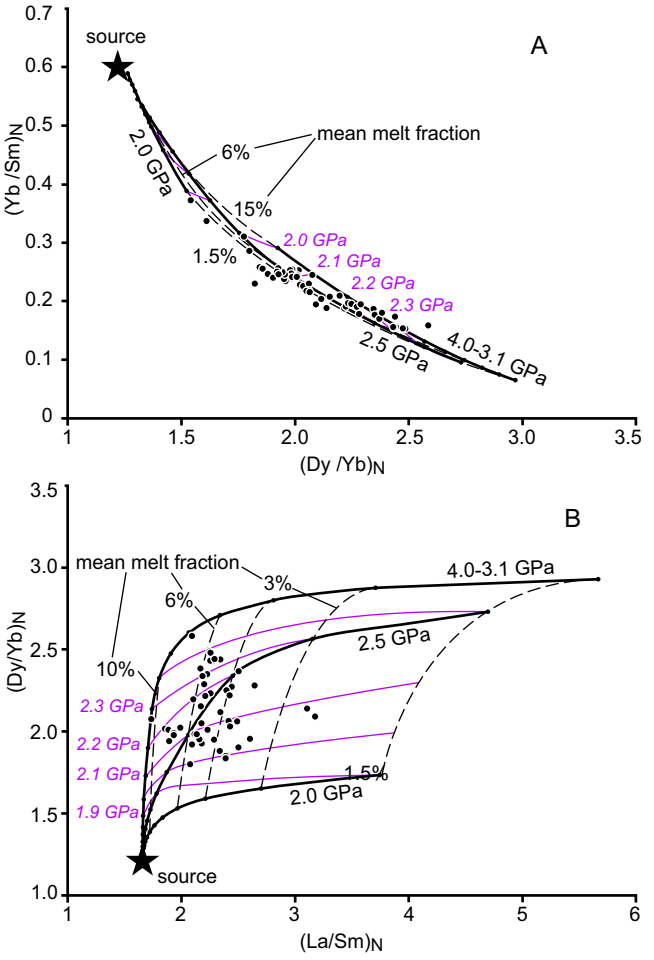

Figure 6. Melting model (a) of $(Dy/Yb)_N$ and $(Yb/Sm)_N$ and (b) $(Dy/Yb)_N$ and $(La/Sm)_N$, for various amounts of partial melting of a peridotitic source, using the REEBOX algorithm of *Fram and Lesher* [1993] and *Fram et al.* [1998]. Black dots represent our LSC data. Different heavy solid curves represent modeled compositions for melting starting at pressures of 4.0 to 3.1, 2.5, and 2 GPa. Pressure at the top of the melting region is indicated by purple curves (labels in italics). Each increment of 0.1 GPa of decompression is assumed to produce a 1.5% melt fraction. Dashed curves represent lines of equal melt fraction. Star represents starting source composition. Normalizing values are those of *Lyubetskaya and Korenaga* [2007].

Figure 6 shows the results of several models in terms of primitive-mantle-normalized $(Dy/Yb)_N$, $(Yb/Sm)_N$, and $(La/Sm)_N$. These elements are highly to moderately incompatible in mafic systems, resistant to alteration and, in the case of Yb and Dy, compatible in garnet, which permits a test for the presence of garnet in the source. The best fit to our data is achieved with a source composition somewhat enriched in LREE (light rare earth elements), with starting $(Dy/Yb)_N = 1.22$, $(Yb/Sm)_N = 0.61$, and $(La/Sm)_N = 1.67$. Use of other commonly used partition coefficients does not greatly change this result (e.g., those in *Green*'s [1994] compilation yield values of 1.21, 0.67, and 1.40, respectively). A LREE-enriched source is also required by other melting models, such as batch and monobaric aggregated fractional melting [*Shaw*, 1970]. A LREE-enriched immediate source for LSC lavas contrasts with their positive ε_{Nd} values, which indicate a time-averaged source depletion of Nd relative to Sm. Rather than representing a hypothetical recent LREE enrichment event of the LSC source rocks, this discrepancy more likely results from complexities of the source mineralogy, and of melt extraction and aggregation processes [e.g., *Stracke and Bourdon*, 2009] that are not adequately accounted for in REEBOX.

Aggregate melt fractions estimated from Figure 6 are mostly between 2% and 7% (but range as high as 13% for one sample), corresponding to 0.1–0.5 GPa of decompression (i.e., over a depth interval of ~15 km). Our data necessitate polybaric melting conditions, with much of the melting occurring in the presence of garnet. Model results for starting pressures ≥3.1 GPa are essentially indistinguishable and all yield acceptable fits. These results are in good agreement with our estimates of roughly 90–110 km thick lithosphere (pressures of ~3.0–3.7 GPa) at the time of emplacement of the majority of seamounts (Table 1).

5.3. Systematic Geochemical Variations With Time and Lithosphere Thickness

Our data, combined with those of *Cheng et al.* [1987] and *Beier et al.* [2011], show no systematic temporal isotopic variation with indicators of either the degree of magmatic evolution or partial melting, with the full range of compositions being observed at a single volcano (e.g., Figure 7). In addition, no correlation is observed between age-corrected isotopic ratios or incompatible element ratios and the estimated seafloor age or thickness of the lithosphere at the time of seamount emplacement (Figure 8). As noted earlier, there is also no discernable systematic variation of either chemical or isotopic composition with distance from the

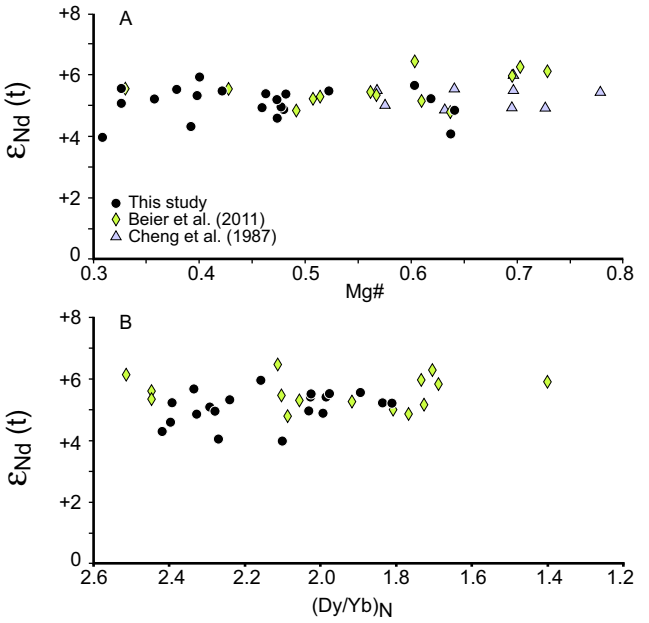

Figure 7. Variation of $\varepsilon_{Nd}(t)$ with geochemical indicators of (a) fractionation indices (Mg#) and (b) degree of partial melting $(Dy/Yb)_N$. Normalizing values are those of *Lyubetskaya and Korenaga* [2007].

hot spot (volcano age) over the last ~50 Myr; that is, east of the western arm of the Wishbone Scarp (Figure 9), despite the abrupt drop in magma productivity over the past 25 Myr. These results suggest that the small isotopic variations observed are more likely to be related to slight variability in source composition (relative to the length-scale of melting) than to variations in melting conditions. Indeed, variations in melting conditions would be expected to cause some components in an heterogeneous source (such as pyroxenite or eclogite lithologies) to be expressed more than others as a function of relative fusibility [cf., *Ito and Mahoney*, 2005a, 2005b], which we do not observe (Figures 7 and 8). Samples from dredge 20D, which were all collected from the same seamount, show a significant range in isotopic composition (Figures 8 and 9), which may also favor the former hypothesis, as lithospheric thickness is unlikely to vary substantially under a single seamount during its construction—assuming a relatively short construction time. *Koppers et al.* [2011] reported a total age range of 1.6 Myr among samples from dredge 20D.

Beier et al. [2011] reported preliminary data suggesting that some Louisville seamounts had protracted life spans, but these results were not confirmed by *Koppers et al.* [2011]. As a result, we take the unpublished, anomalously young ages for the "very late-stage" SO167 samples in *Beier et al.* [2011, Figure 6] to be inaccurate. Consequently, the low Nb/Zr and La/Yb of some lavas from the westernmost Louisville Seamounts [see *Beier et al.*, 2011, Figures 5b and 8b] are unlikely to represent a later stage of more depleted magmatism. These low trace element ratios may be affected by the proximity of young, thin lithosphere close to the Osbourn Trough, though isotopic ratios do not appear to be similarly affected.

Along most of the LSC, lack of correlation of isotopic ratios with estimated lithospheric thickness at the time of seamount emplacement suggests that the small variations in lithospheric thickness were not the dominant factor controlling isotopic variation. Furthermore, $(Dy/Yb)_N$ and other heavy rare earth element ratios in the samples of dredge 20D do not correlate with isotopic ratios, indicating that there was not much difference in the fusibility of isotopically different zones or components within the mantle source (such as pyroxenite or eclogite lithologies)—again assuming the lavas recovered in dredge 20D were erupted relatively close in time. For comparison, volcanoes of some other hot spots, such as the Cook-Austral, Society and Pitcairn, have also been emplaced on crust of relatively constant age [*Müller et al.*, 2008], yet display much wider ranges in isotopic compositions than observed for the LSC [e.g., *Devey et al.*, 1990; *Cotten et al.*, 1995; *Lassiter et al.*, 2003].

In summary, our results indicate that the Louisville source mantle has long been unusually homogeneous. Assuming the Louisville hot spot is produced by a mantle plume, the implication is that the plume originates from a "well-stirred" or "pure" portion of the mantle.

5.4. The Louisville Hot Spot as the Source of the Ontong Java Plateau

The plume head of the Louisville hot spot has been suggested as a candidate for the source of the ~120 Ma Ontong Java Plateau (OJP) [e.g., *Mahoney*, 1987; *Mahoney and Spencer*, 1991; *Richards et al.*, 1991; *Tarduno et al.*, 1991] and, by extension, of the Hikurangi and Manihiki plateaus, postulated to

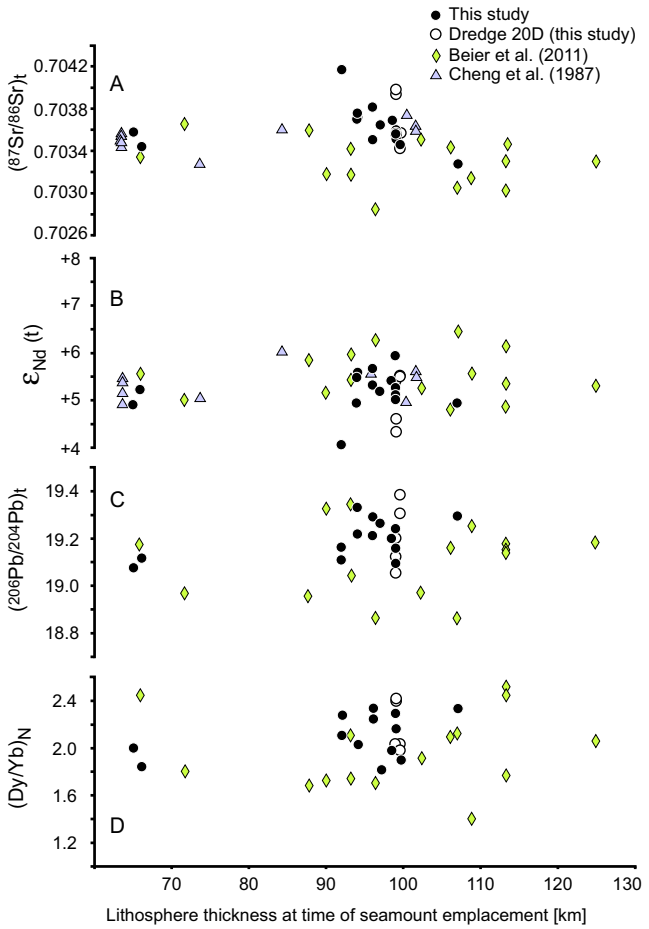

Figure 8. Variation of (a–c) isotopic ratios and (d) $(Dy/Yb)_N$, as a function of estimated lithospheric thickness at the time of seamount volcanism. Lithosphere thickness is determined using crustal age at time of volcanism and a half-space lithospheric cooling model [*Turcotte and Schubert*, 1982]. Data for highly altered samples are not included. Normalizing values are those of *Lyubetskaya and Korenaga* [2007].

have rifted from the OJP [*Taylor*, 2006; *Worthington et al*., 2006]. Because portions of the Louisville hot spot trail older than about 80 Ma have been subducted at the Tonga-Kermadec Trench [*Timm et al*., 2013], it is, to a large degree, not possible to backtrack the hot spot from its earlier seafloor record. Most recent plate motion models [e.g., *Wessel and Kroenke*, 2008] fail to place the hot spot in the vicinity of the OJP at ~120 Ma, although *Antretter et al*. [2004] concluded that the latitudinal discrepancy between the inferred present location of the Louisville hot spot and the estimated original location of the OJP can be accommodated by allowing for a combination of true polar wander, long-term octupole components of the geomagnetic field, and post-OJP southward motion of the Louisville hot spot. *Chandler et al*. [2012] reach similar conclusions. However, paleomagnetic data for IODP Expedition 330 samples from guyots younger than 70 Ma [*Koppers et al*., 2012a, 2012b], and the lack of large changes in the Louisville-Hawai'i interchain distance [*O'Connor et al*., 2013] are compatible with relatively little latitudinal hot spot motion from its present position.

Our Nd and Sr isotopic data for LSC lavas overlap with values for the OJP basalts. However, the Pb isotopic compositions are distinct from those of either of the two principal OJP magma types, the Kwaimbaita and Singgalo [e.g., *Mahoney et al*., 1993; *Tejada et al*., 2004], and post-120 Ma isotopic evolution of Pb in the LSC mantle source from decay of Th and U cannot account for the differences. The slope of the age-correction (evolution) vector for the LSC data in $^{206}Pb/^{204}Pb$ versus $^{207}Pb/^{204}Pb$ space (Figure 10) depends upon the present-day $^{238}U/^{235}U$ ratio, 137.88, which varies little in natural materials in the solar system. This vector not only fails to intersect the OJP data fields, but would also require very high $^{238}U/^{204}Pb$ ($=\mu$) values (40–80) in the mantle source in order to explain the difference in age-corrected $(^{206}Pb/^{204}Pb)_t$ between the LSC and OJP rocks. Such μ values are higher than measured in almost all LSC samples, with 90% of those we analyzed having a μ value between 15 and 43. Further, because U is more incompatible than Pb in mantle rocks [e.g., *Tatsumoto*, 1988] and the LSC lavas appear to be products of relatively small amounts of partial melting, μ must be lower in the Louisville mantle source than in LSC magmas. In addition, OJP compositions cannot be produced by mixing LSC-type and EPR-type isotopic mantle end-members. Interlaboratory measurement bias also cannot explain the discrepancy between the LSC evolution vector and OJP compositions, as the great majority of the OJP (and some Manihiki) isotopic data were acquired in the same laboratory as that used in the present study, and include a number of Pb double-spike measurements [*Tejada et al*., 2004].

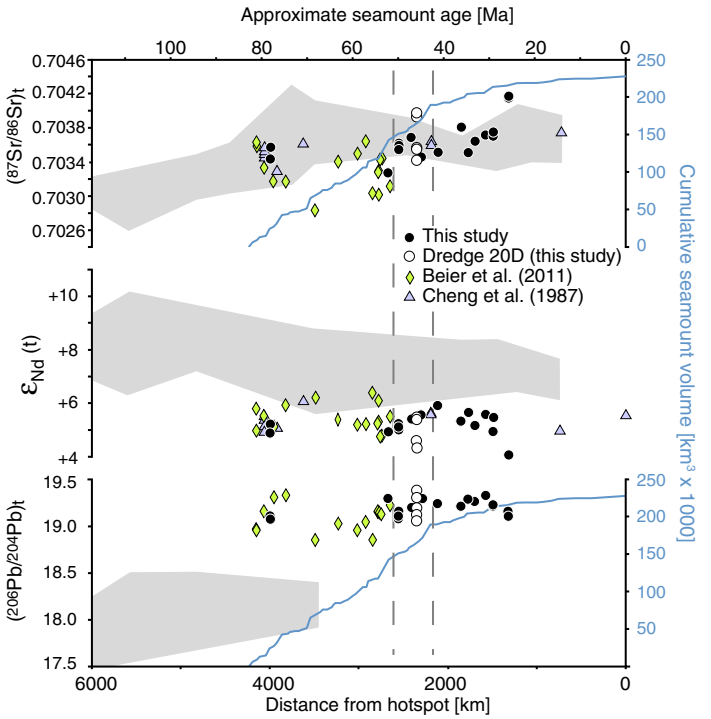

Figure 9. Along-chain isotopic variation with distance from the hot spot (assumed to be at 50°26.4′S, 139°10′W, the site of dredge MTHN-7D) [*Lonsdale*, 1988]. Dashed lines show the locations of the western and eastern branches of the Wishbone Scarp. Blue line represents the cumulative seamount volume curve, based on data from *Lonsdale* [1988] and the Seamount Catalog (available at http://earthref.org) [*Koppers et al.*, 2010]. Data for highly altered samples are not included. Data from the Hawai'i-Emperor chain are shown as a gray field for comparison [*Lanphere et al.*, 1980; *Basu and Faggart*, 1996; *Keller et al.*, 2000; *Regelous et al.*, 2003; *Frey et al.*, 2005; *Huang et al.*, 2005; *Shafer et al.*, 2005].

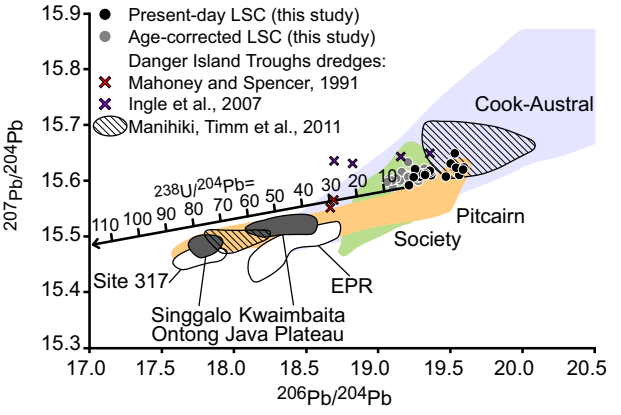

Figure 10. Comparison of LSC $^{207}Pb/^{204}Pb$-$^{206}Pb/^{204}Pb$ values with age-adjusted fields for the two principal magma types of OJP basalts (Kwaimbaita and Singgalo), for cored basalts from the Manihiki Plateau at Deep Sea Drilling Project Site 317, and for samples dredged at multiple locations of the Manihiki Plateau. Age-corrected values of dredged basalts from the Danger Islands Troughs of the Manihiki Plateau are noted by red [*Mahoney and Spencer*, 1991] (age correction uses the U, Th, and Pb concentrations in *Ingle et al.* [2007, Table DR-4]) and purple Xs [*Ingle et al.*, 2007]. Black dots represent the present-day values of our LSC samples, and gray dots correspond to the age-corrected values. Measurement error on LSC analyses is less than or equal to symbol size. The $^{238}U/^{204}Pb$ (μ) vector represents the effect for different values of μ (indicated by tick marks) of age-correcting the LSC isotopic ratios to 120 Ma. Site 317 field is from *Hoernle et al.* [2010]. East Pacific Rise (EPR) field corresponds to present-day data from 13.4 to 23°S axis [after *Bach et al.*, 1994; *Mahoney et al.*, 1994; *Niu et al.*, 1996]. Ontong Java Plateau data are from *Mahoney et al.* [1993] and *Tejada et al.* [1996, 2002, 2004]. Manihiki Plateau data (striped fields) are from *Timm et al.* [2011]. Fields for other Pacific hot spots are from data sources in Figure 5.

Few isotopic data have been published for the Hikurangi Plateau [*Mortimer and Parkinson*, 1996; *Hoernle et al.*, 2010], but those that are available are rather similar to those for the two main types of OJP basalt and thus also distinct from Louisville compositions. Likewise, the $^{207}Pb/^{204}Pb$ and $^{206}Pb/^{204}Pb$ ratios of LSC lavas are also too high to have evolved from the compositions measured for the Manihiki Plateau lavas drilled at Deep Sea Drilling Project Site 317, which are similar to the Singgalo magma type of the OJP (Figure 10). Recently, *Timm et al.* [2011] discovered a set of low-Ti, FOZO-like Manihiki samples with much higher $^{206}Pb/^{204}Pb$ than had ever been previously reported—so

high, in fact, that the LSC mantle source could not have evolved from the source of Manihiki low-Ti lavas either (Figure 10).

Of course, we cannot rule out the possibility of a shift in the isotopic composition of lavas between the plume-head and plume-tail stage of the hot spot. Such a change would not be unexpected, considering the very high degrees of partial melting estimated for OJP and Manihiki Site 317 basalts (18–30%) [*Mahoney et al*., 1993; *Tejada et al*., 1996; *Neal et al*., 1997; *Fitton and Godard*, 2004; *Herzberg*, 2004], which could have swamped any LSC-like isotopic signal produced by the melting of relatively fusible, but volumetrically minor, material in the source. Less speculatively, age-corrected data for two glassy samples from a dredge haul in the Danger Islands Troughs (red Xs in Figure 10) of the Manihiki Plateau [*Mahoney and Spencer*, 1991; *Ingle et al*., 2007] fall on the LSC Pb evolution vector in Figure 10. These samples also have LSC-like Nd and Sr isotopic values. Therefore, assuming that the Manihiki Plateau is a rifted fragment of the OJP, a genetic link between the Louisville hot spot and the OJP remains possible on this narrow basis.

6. Conclusions

We selected dredge sites to target mainly shield-stage lavas along the LSC. Yet most of our samples are chemically and isotopically very similar to those described by *Hawkins et al*. [1987] and *Cheng et al*. [1987], which were also Si-unsaturated. Like *Beier et al*. [2011], we tentatively conclude that Louisville volcanoes lack compositionally distinct shield and postshield stages. The same conclusion appears to apply to lavas drilled recently at four LSC seamounts [*Koppers et al*., 2012a].

Major and compatible trace elements show patterns consistent with the fractionation of an olivine+clinopyroxene (±plagioclase) mineral assemblage. Incompatible trace elements indicate that the melts were partly, and in many cases largely, formed in the garnet stability zone. Modeling indicates that low degrees of partial melting (2–7%) of a likely peridotitic source can explain the observed range of rare earth characteristics. Isotopic data reveal that the source was C/FOZO-like. The small range of isotopic compositions along the LSC sets it apart from other Pacific hot spot tracks. The Louisville mantle source appears to have remained unusually homogeneous over at least the last ~70 Myr. Magma fluxes from the hot spot have decreased sharply in the past 25 Myr [*Lonsdale*, 1988; *Koppers et al*., 2011], but this appears not to have been accompanied by any significant change in chemical or isotopic composition of Louisville lavas, indicating that the source and melting conditions have remained much the same, while upwelling rates may have decreased. The lack of systematic along-chain variation is epitomized by the fact that nearly the entire range of geochemical characteristics exhibited by LSC lavas over the last ~50 Myr are observed in samples from a single seamount (Dredge 20D).

The small isotopic variations that are present appear unrelated to the degree of partial melting or magmatic evolution. Nor is any correlation observed between isotopic characteristics and estimated lithospheric thickness at the time of volcanism, with the exception of the oldest, westernmost Louisville Seamounts which erupted lavas with lower Nb/Zr and La/Yb, and which were formed close to the actively spreading Osbourn Trough. This result suggests that isotopic variability was not controlled by changes in melting conditions, but instead by the amount of minor, isotopically distinct heterogeneities present in the melting zone at a given time. The absence of correlation between isotopic ratios and indicators of degree of partial melting also implies that isotopically different volumes of the mantle source had broadly similar fusibility.

The Louisville isotopic signature has not been found in OJP basalts, Hikurangi Plateau lavas, or drilled Manihiki Plateau basalts, and cannot have evolved from a source with the signatures of those lavas. We cannot completely discount the Louisville hot spot as the source of these Cretaceous Pacific plateau basalts, but it would require one of two things. One is an isotopic shift in source composition between the plume head and plume tail stages of activity. Such a change would be particularly striking in light of the overall homogeneity of Louisville lavas for the past ~70 Myr [cf. *Mahoney*, 1987]. Alternatively, the isotopic differences may be attributed to the very different degrees of partial melting inferred for LSC (generally only a few percent) versus OJP and Manihiki (18–30%) lavas, such that more-refractory mantle components in the source dominated plateau lava compositions but are not expressed significantly in the LSC. Intriguingly, the $^{207}Pb/^{204}Pb$-$^{206}Pb/^{204}Pb$ evolution vector for the Louisville seamounts intersects the Pb isotopic values of some dredged lavas from the Danger Islands Troughs of the Manihiki Plateau,

which also have LSC-like Sr and Nd isotopic ratios. This similarity is consistent with, but not proof of, a stronger link between the Louisville hot spot and the OJP than suggested by most recent plate motion models.

Acknowledgments

We thank B. Eakins, R. Comer, and the captain and crew of the R.V. Revelle for their invaluable work during the AMAT expedition. D. Pyle assisted in the laboratory, and he and G. Ito provided extensive reviews of early drafts of the manuscript. G. Gordon is thanked for her generosity in helping acquire additional Sr data. T. Bianco, D. Buchs, M. Garcia, S. Ingle, E. Mittelstaedt, and R. Workman offered helpful comments, and we thank C. Timm, D. Geist, M. Rhodes, and two anonymous reviewers for their careful evaluation of the manuscript. The authors gratefully acknowledge the support of the US National Science Foundation (grants OCE04-52127 and OCE03-51512).

References

Abouchami, W., S. J. G. Galer, and A. W. Hofmann (2000), High precision lead isotope systematics of lavas from the Hawaiian scientific drilling project, *Chem. Geol.*, *169*, 187–209.

Abouchami, W., A. W. Hofmann, S. J. G. Galer, F. A. Frey, J. Eisele, and M. Feigenson (2005), Lead isotopes reveal bilateral asymmetry and vertical continuity in the Hawaiian mantle plume, *Nature*, *434*, 851–856, doi:10.1038/nature03402.

Antretter, M., P. Riisager, S. Hall, X. Zhao, and B. Steinberger (2004), Modeled paleolatitudes for the Louisville hotspot and the Ontong Java Plateau, in *Origin and Evolution of the Ontong Java Plateau, Spec. Publ. 229*, edited by J. G. Fitton, et al., pp. 21–30, Geol. Soc. of London, London, U. K.

Bach, W., E. Hegner, J. Erzinger, and M. Satir (1994), Chemical and isotopic variations along the superfast spreading East Pacific Rise from 6° to 30°S, *Contrib. Mineral. Petrol.*, *116*, 365–380.

Baker, P. E., F. Buckley, and J. G. Holland (1974), Petrology and geochemistry of Easter Island, *Contrib. Mineral. Petrol.*, *44*, 85–100.

Basu, A. R., and B. E. Faggart (1996), Temporal variation in the Hawaiian Mantle Plume: The Lanai Anomaly, The Molokai Fracture Zone and a seawater-altered lithospheric component in Hawaiian Volcanism, in *Earth Processes: Reading the Isotopic Code, Geophys. Monogr. Ser. 95*, pp. 149–159, AGU, Washington, D. C.

Baturin, G., and I. Yushina (2007), Rare earth elements in phosphate-ferromanganese crusts on Pacific seamounts, *Lithol. Mineral Resour.*, *42*(2), 101–117.

Beier, C., L. Vanderkluysen, M. Regelous, J. J. Mahoney, and D. Garbe-Schönberg (2011), Lithospheric control on geochemical composition along the Louisville Seamount Chain, *Geochem. Geophys. Geosyst.*, *12*, Q0AM01, doi:10.1029/2011GC003690.

Belousova, E., W. Griffin, S. Y. O'Reilly, and N. Fisher (2002), Igneous zircon: Trace element composition as an indicator of source rock type, *Contrib. Mineral. Petrol.*, *143*(5), 602–622.

Bence, A. E., S. R. Taylor, and M. Fisk (1980), Major and trace-element geochemistry of basalts from Ojin, Nintoku, and Suiko seamounts of the Emperor seamount chain, DSDP-IPOD leg 55, *Initial Rep. Deep Sea Drill. Proj.*, *55*, 599–605.

Blichert-Toft, J., and F. Albarède (2009), Mixing of isotopic heterogeneities in the Mauna Kea plume conduit, *Earth Planet. Sci. Lett.*, *282*(1–4), 190–200, doi:10.1016/j.epsl.2009.03.015.

Blichert-Toft, J., D. Weis, C. Maerschalk, A. Agranier, and F. Albarède (2003), Hawaiian hot spot dynamics as inferred from the Hf and Pb isotope evolution of Mauna Kea volcano, *Geochem. Geophys. Geosyst.*, *4*(2), 8704, doi:10.1029/2002GC000340.

Bonatti, E., C. G. A. Harrison, D. E. Fisher, J. Honnorez, J.-G. Schilling, J. J. Stipp, and M. Zentilli (1977), Easter volcanic chain (Southeast Pacific): A mantle hot line, *J. Geophys. Res.*, *82*(17), 2457–2478.

Boyet, M., and R. W. Carlson (2006), A new geochemical model for the Earth's mantle inferred from ^{146}Sm-^{142}Nd systematics, *Earth Planet. Sci. Lett.*, *250*, 254–268.

Cambon, P., J.-L. Joron, H. Bougault, and M. Treuil (1980), Leg 55, Emperor seamounts: Trace elements in transitional tholeiities, alkali basalts and hawaiites—Mantle homogeneity or heterogeneity and magmatic processes, *Initial Rep. Deep Sea Drill. Proj.*, *55*, 585–597.

Chandler, M. T., P. Wessel, B. Taylor, M. Seton, S.-S. Kim, and K. Hyeong (2012), Reconstructing Ontong Java Nui: Implications for Pacific absolute plate motion, hotspot drift and true polar wander, *Earth Planet. Sci. Lett.*, *331–332*, 140–151, doi:10.1016/j.epsl.2012.03.017.

Chauvel, C., W. F. McDonough, G. Guille, R. Maury, and R. A. Duncan (1997), Contrasting old and young volcanism in Rurutu island, Austral chain, *Chem. Geol.*, *139*, 125–143.

Chen, C.-Y., and F. A. Frey (1985), Trace element and isotopic geochemistry of lavas from Haleakala volcano, East Maui, Hawaii: Implications for the origin of Hawaiian basalts, *J. Geophys. Res.*, *90*(B10), 8743–8768.

Chen, C.-Y., F. A. Frey, and M. O. Garcia (1990), Evolution of alkalic lavas at Haleakala volcano, East Maui, Hawaii: Major, trace element, and isotopic constraints, *Contrib. Mineral. Petrol.*, *105*, 197–218.

Chen, C.-Y., F. A. Frey, J. M. Rhodes, and R. M. Easton (1996), Temporal geochemical evolution of Kilauea volcano: Comparison of Hilina and Puna basalt, in *Earth Processes: Reading the Isotopic Code, Geophys. Monogr. Ser. 95*, edited by A. Basu and S. R. Hart, pp. 161–181, AGU, Washington, D. C.

Cheng, Q., K.-H. Park, J. D. Macdougall, A. Zindler, G. W. Lugmair, H. Staudigel, J. Hawkins, and P. Lonsdale (1987), Isotopic evidence for a hotspot origin of the Louisville seamount chain, in *Seamounts, Islands, and Atolls, Geophys. Monogr. Ser. 43*, edited by B. H. Keating, et al., pp. 283–296, AGU, Washington, D. C.

Cheng, Q. C., J. D. Macdougall, and G. W. Lugmair (1993), Geochemical studies of Tahiti and Mehetia, Society island chain, *J. Volcanol. Geothermal Res.*, *55*, 155–184.

Clague, D. A., and R. D. Jarrard (1973), Tertiary plate motion deduced from the Hawaii-Emperor chain, *Bull. Geol. Soc. Am.*, *84*, 1135–1154.

Contreras-Reyes, E., I. Grevemeyer, A. B. Watts, L. Planert, E. R. Flueh, and C. Peirce (2010), Crustal intrusion beneath the Louisville hotspot track, *Earth Planet. Sci. Lett.*, *289*, 323–333.

Cotten, J., A. Le Dez, M. Bau, M. Caroff, R. C. Maury, P. Dulski, S. Fourcade, M. Bohn, and R. Brousse (1995), Origin of anomalous rare-earth element and yttrium enrichments in subaerially exposed basalts: Evidence from French Polynesia, *Chem. Geol.*, *119*, 115–138.

Cottrell, R. D., and J. A. Tarduno (2003), A Late cretaceous pole for the Pacific plate: Implications for apparent and true polar wander and the drift of hotspots, *Tectonophysics*, *362*, 321–333.

Dalrymple, G. B., D. A. Clague, M. O. Garcia, and S. W. Bright (1981), Petrology and K-Ar ages of dredged samples from Laysan Island and Northampton Bank volcanoes, Hawaiian ridge, and evolution of the Hawaiian-Emperor chain, *Bull. Geol. Soc. Am. Part II*, *92*, 884–933.

Dasgupta, R., M. M. Hirschmann, and K. Stalker (2006), Immiscible transition from carbonate-rich to silicate-rich melts in the 3 GPa melting interval of eclogite + CO_2 and genesis of silica-undersaturated Ocean Island Lavas, *J. Petrol.*, *47*(4), 647–671, doi:10.1093/petrology/egi088.

Dasgupta, R., M. M. Hirschmann, and N. D. Smith (2007), Partial melting experiments of peridotite + CO_2 at 3 GPa and genesis of alkalic ocean island basalts, *J. Petrol.*, *48*(11), 2093–2124, doi:10.1093/petrology/egm053.

De Carlo, E. H., G. M. McMurtry, and K. H. Kim (1987), Geochemistry of ferromanganese crusts from the Hawaiian Archipelago—I. Northern survey areas, *Deep Sea Res., Part A*, *34*(3), 441–467.

Devey, C. W., F. Albarède, J.-L. Cheminée, A. Michard, R. Mühe, and P. Stoffers (1990), Active submarine volcanism on the Society hotspot swell (west Pacific): A geochemical study, *J. Geophys. Res.*, *95*(B4), 5049–5066.

Downey, N. J., J. M. Stock, R. W. Clayton, and S. C. Cande (2007), History of the Cretaceous Osbourn spreading center, *J. Geophys. Res.*, *112*, B04102, doi:10.1029/2006JB004550.
Dupuy, C., P. Vidal, R. C. Maury, and G. Guille (1993), Basalts from Mururoa, Fangataufa, and Gambier islands (French Polynesia); geochemical dependence on the age of the lithosphere, *Earth Planet. Sci. Lett.*, *117*, 89–100.
Eisele, J., W. Abouchami, S. J. G. Galer, and A. W. Hofmann (2003), The 320 kyr Pb isotope evolution of Mauna Kea lavas recorded in the HSDP-2 drill core, *Geochem. Geophys. Geosyst.*, *4*(5), 8710, doi:10.1029/2002GC000339.
Fitton, J. G., and M. Godard (2004), Origin and evolution of magmas on the Ontong Java Plateau, in *Origin and Evolution of the Ontong Java Plateau, Spec. Publ. 229*, edited by J. G. Fitton, et al., pp. 151–178, Geol. Soc. of London, London, U. K.
Fitton, J. G., A. D. Saunders, M. J. Norry, B. S. Hardarson, and R. N. Taylor (1997), Thermal and chemical structure of the Iceland plume, *Earth Planet. Sci. Lett.*, *153*(3–4), 197–208.
Fram, M. S., and C. E. Lesher (1993), Geochemical constraints on mantle melting during creation of the North Atlantic basin, *Nature*, *363*, 712–715.
Fram, M. S., C. E. Lesher, and A. M. Volpe (1998), Mantle melting systematics: Transition from continental to oceanic volcanism on the southeast Greenland margin, in *Proceedings of Ocean Drilling Program, Scientific Results*, vol. 152, edited by A. D. Saunders, H. C. Larsen, and S. W. Wise Jr., pp. 373–386, Ocean Drilling Program, College Station, TX, USA.
Frey, F. A., M. O. Garcia, and M. F. Roden (1994), Geochemical characteristics of Koolau volcano, implications of intershield geochemical differences among Hawaiian volcanoes, *Geochim. Cosmochim. Acta*, *58*, 1441–1462.
Frey, F. A., S. Huang, J. Blichert-Toft, M. Regelous, and M. Boyet (2005), Origin of depleted components in basalt related to the Hawaiian hot spot: Evidence from isotopic and incompatible element ratios, *Geochem. Geophys. Geosyst.*, *6*, Q02L07, doi:10.1029/2004GC000757.
Galer, S. J. G. (1999), Optimal double and triple spiking for high precision lead isotopic measurement, *Chem. Geol.*, *157*(3–4), 255–274.
Green, T. H. (1994), Experimental studies of trace element partitioning applicable to petrogenesis—Sedona 16 years later, *Chem. Geol.*, *117*, 1–36.
Haase, K. M. (1996), The relationship between the age of the lithosphere and the composition of oceanic magmas: Constraints on partial melting, mantle sources and the thermal structure of the plates, *Earth Planet. Sci. Lett.*, *144*, 75–92.
Haase, K. M., P. Stoffers, and C. D. Garbe-Schönberg (1997), The petrogenetic evolution of lavas from Easter Island and neighbouring seamounts, near-ridge hotspot volcanoes in the SE Pacific, *J. Petrol.*, *38*, 785–813.
Hanan, B. B., and D. W. Graham (1996), Lead and helium isotope evidence from oceanic basalts for a common deep source of mantle plumes, *Science*, *272*, 991–995.
Hart, S. R., E. H. Hauri, L. A. Oschmann, and J. A. Whitehead (1992), Mantle plumes and entrainment: Isotopic evidence, *Science*, *256*, 517–520.
Hauri, E. H., J. C. Lassiter, and D. J. DePaolo (1996), Osmium isotope systematics of drilled lavas from Mauna Loa, *Hawaii*, J. Geophys. Res., *101*(B5), 11,793–11,806.
Hawkins, J. W. (1973), Louisville Ridge, *Eos Trans. AGU*, *54*, 1212.
Hawkins, J. W., P. F. Lonsdale, and R. Batiza (1987), Petrologic evolution of the Louisville seamount chain, in *Seamounts, Islands, and Atolls, Geophys. Monogr. Ser. 43*, edited by B. H. Keating, et al., pp. 235–254, AGU, Washington, D. C.
Hayes, D. E., and M. Ewing (1971), The Louisville ridge—A possible extension of the Eltanin fracture zone, in *Antarctic Oceanology I, Antarct. Res. Ser. 15*, edited by J. L. Reid, pp. 223–228, AGU, Washington, D. C.
Hemond, C., C. W. Devey, and C. Chauvel (1994), Source compositions and melting processes in the Society and Austral plumes (South Pacific Ocean); element and isotope (Sr, Nd, Pb, Th) geochemistry, *Chem. Geol.*, *115*, 7–45.
Herzberg, C. (2004), Partial melting below the Ontong Java Plateau, in *Origin and Evolution of the Ontong Java Plateau, Spec. Publ.*, vol. 229, edited by J. G. Fitton et al., pp. 179–184, Geol. Soc. of London, London, U. K.
Hirschmann, M. M., T. Kogiso, M. B. Baker, and E. M. Stolper (2003), Alkalic magmas generated by partial melting of garnet pyroxenite, *Geology*, *31*(6), 481–484, doi:10.1130/0091–7613(2003)031<0481:AMGBPM> 2.0.CO;2.
Hoernle, K., F. Hauff, P. van den Bogaard, R. Werner, N. Mortimer, J. Geldmacher, D. Garbe-Schönberg, and B. Davy (2010), Age and geochemistry of volcanic rocks from the Hikurangi and Manihiki oceanic Plateaus, *Geochim. Cosmochim. Acta*, *74*, 7196–7219.
Hofmann, A. W. (1988), Chemical differentiation of the Earth: The relationship between mantle, continental crust, and oceanic crust, *Earth Planet. Sci. Lett.*, *90*(3), 297–314, doi:10.1016/0012–821X(88)90132-X.
Hofmann, A. W., and W. M. White (1982), Mantle plumes from ancient oceanic crust, *Earth Planet. Sci. Lett.*, *57*, 421–436.
Hole, M. J., A. D. Saunders, G. F. Marriner, and J. Tarney (1984), Subduction of pelagic sediments: Implications for the origin of Ce-anomalous basalts from the Mariana Islands, *J. Geol. Soc. London*, *141*(3), 453–472.
Hoskin, P. W. O., and U. Schaltegger (2003), The composition of zircon and igneous and metamorphic petrogenesis, *Rev. Mineral. Geochem.*, *53*, 27–62.
Huang, S., M. Regelous, T. Thordarson, and F. A. Frey (2005), Petrogenesis of lavas from Detroit seamount: Geochemical differences between Emperor chain and Hawaiian volcanoes, *Geochem. Geophys. Geosyst.*, *6*, Q01L06, doi:10.1029/2004GC000756.
Humphries, S. E., and G. Thompson (1978), Hydrothermal alteration of oceanic basalts by seawater, *Geochim. Cosmochim. Acta*, *42*, 107–125.
Ingle, S., J. J. Mahoney, H. Sato, M. F. Coffin, J.-I. Kimura, N. Hirano, and M. Nakanishi (2007), Depleted mantle wedge and sediment fingerprint in unusual basalts from the Manihiki Plateau, central Pacific Ocean, *Geology*, *35*(7), 595–598, doi:10.1130/G23741A.1.
Ingram, B. L., J. R. Hein, and G. L. Farmer (1990), Age determinations and growth rates of Pacific ferromanganese deposits using strontium isotopes, *Geochim. Cosmochim. Acta*, *54*, 1709–1721.
Ito, G., and J. J. Mahoney (2005a), Flow and melting of a heterogeneous mantle: 1. Method and importance to the geochemistry of ocean island and mid-ocean ridge basalts, *Earth Planet. Sci. Lett.*, *230*(1–2), 29–46.
Ito, G., and J. J. Mahoney (2005b), Flow and melting of a heterogeneous mantle: 2. Implications for a chemically nonlayered mantle, *Earth Planet. Sci. Lett.*, *230*(1–2), 47–63.
Jackson, M. C., F. A. Frey, M. O. Garcia, and R. A. Wilmoth (1999), Geology and geochemistry of basaltic lava flows and dikes from the Trans-Koolau tunnel, Oahu, Hawaii, *Bull. Volcanol.*, *60*, 381–401.
Johnson, D. M., P. R. Hooper, and R. M. Conrey (1999), XRF analysis of rocks and minerals for major and trace elements on a single low dilution Li-tetraborate fused bead, in *Proceedings of Denver X-ray Conference on Advances in X-ray Analysis*, vol. 41, edited by B. Clemens et al., pp. 843–867, JCPDS—International Center for Diffraction Data, Newton Square, Pa, USA.
Jurdy, D. M. (1978), An alternative model for early Tertiary absolute plate motions, *Geology*, *6*, 469–472.
Kawakatsu, H., P. Kumar, Y. Takei, M. Shinohara, T. Kanazawa, E. Araki, and K. Suyehiro (2009), Seismic evidence for sharp lithosphere-asthenosphere boundaries of oceanic plates, *Science*, *324*(5926), 499–502, doi:10.1126/science.1169499.

Keller, R. A., M. R. Fisk, and W. M. White (2000), Isotopic evidence for Late Cretaceous plume-ridge interaction at the Hawaiian hotspot, *Nature*, *405*, 673–676.
Kellogg, J. B., S. B. Jacobsen, and R. J. O'Connell (2004), Mantle isotopic heterogeneity: The FOZO's in the pudding, *Eos Trans. AGU*, *85*(17), Jt. Assem. Suppl., Abstract V43A-12.
Knaack, C., S. B. Cornelius, and P. R. Hooper (1994), Trace element analyses of rocks and minerals by ICP-MS, technical notes, GeoAnalytical Lab., Washington St. Univ., Pullman, Wash.
Koppers, A. A. P., R. A. Duncan, and B. Steinberger (2004), Implications of a nonlinear $^{40}Ar/^{39}Ar$ age progression along the Louisville seamount trail for models of fixed and moving hot spots, *Geochem. Geophys. Geosyst.*, *5*, Q06L02, doi:10.1029/2003GC000671.
Koppers, A. A. P., H. Staudigel, and R. Minnett (2010), Seamount catalog: Seamount morphology, maps, and data files, *Oceanography*, *23*(1), 37, doi:10.5670/oceanog.2010.88.
Koppers, A. A. P., M. D. Gowen, L. E. Colwell, J. S. Gee, P. F. Lonsdale, J. J. Mahoney, and R. A. Duncan (2011), New $^{40}Ar/^{39}Ar$ age progression for the Louisville hot spot trail and implications for inter-hot spot motion, *Geochem. Geophys. Geosyst.*, *12*, Q0AM02, doi:10.1029/2011GC003804.
Koppers, A. A. P., T. Yamazaki, J. Geldmacher, and Expedition 330 Scientists (2012a), Volume 330 expedition reports: Louisville Seamount Trail, in *Proceedings of Integrated Ocean Drilling Program*, Integrated Ocean Drill. Program Manage. Int., Inc., Tokyo, Japan.
Koppers, A. A. P., et al. (2012b), Limited latitudinal mantle plume motion for the Louisville hotspot, *Nat. Geosci.*, *5*, 911–917, doi:10.1038/ngeo1638.
Koppers, A. A. P., T. Yamazaki, J. Geldmacher, and Expedition 330 Scientific Party (2013), IODP Expedition 330: Drilling the Louisville Seamount Trail in the SW Pacific, *Sci. Drill. 15*, 11–22, doi:10.2204/iodp.sd.15.02.2013.
Lanphere, M. A., et al. (1980), Rb-Sr systematics of basalts from the Hawaiian-Emperor volcanic chain, *Initial Rep. Deep Sea Drill. Proj.*, *55*, 695–706.
Larson, R. L., and C. E. Chase (1972), Late Mesozoic evolution of the western Pacific Ocean, *Geol. Soc. Am. Bull.*, *83*, 3627–3644.
Lassiter, J. C., J. Blichert-Toft, E. H. Hauri, and H. G. Barsczus (2003), Isotope and trace element variations in lavas from Raivavae and Rapa, Cook-Austral islands: Constraints on the nature of HIMU-and EM-mantle and the origin of mid-plate volcanism in French Polynesia, *Chem. Geol.*, *202*, 115–138.
Le Bas, M. J., R. W. Le Maitre, A. Streckeisen, and B. Zanettin (1986), A chemical classification of volcanic rocks on the total alkali–silica diagram, *J. Petrol.*, *27*, 745–750.
Lonsdale, P. (1988), Geography and history of the Louisville hotspot chain in the Southwest Pacific, *J. Geophys. Res.*, *93*(B4), 3078–3104.
Lonsdale, P. (1997), An incomplete geologic history of the south-west Pacific Basin, *Geol. Soc. Am. Abstr. Programs*, *29*, 4574.
Lyons, S. N., D. T. Sandwell, and W. H. F. Smith (2000), Three-dimensional estimation of elastic thickness under the Louisville Ridge, *J. Geophys. Res.*, *105*(B6), 13,239–13,252.
Lyubetskaya, T., and J. Korenaga (2007), Chemical composition of Earth's primitive mantle and its variance: 1. Method and results, *J. Geophys. Res.*, *112*, B03211, doi:10.1029/2005JB004223.
Macdonald, G. A. (1968), Composition and origin of Hawaiian lavas, *Mem. Geol. Soc. Am.*, *116*, 477–522.
Macdonald, G. A., and T. Katsura (1964), Chemical composition of Hawaiian lavas, *J. Petrol.*, *5*(1), 82–133.
Mahoney, J. J. (1987), An isotopic survey of Pacific oceanic plateaus: Implications for their nature and origin, in *Seamounts, Islands, and Atolls, Geophys. Monogr. Ser. 43*, edited by B. H. Keating et al., pp. 207–220, AGU, Washington, D. C.
Mahoney, J. J., and K. J. Spencer (1991), Isotopic evidence for the origin of the Manihiki and Ontong Java oceanic plateaus, *Earth Planet. Sci. Lett.*, *104*, 196–210.
Mahoney, J. J., C. Nicollet, and C. Dupuy (1991), Madagascar basalts: Tracking oceanic and continental sources, *Earth Planet. Sci. Lett.*, *104*, 350–363.
Mahoney, J. J., M. Storey, R. A. Duncan, K. J. Spencer, and M. S. Pringle (1993), Geochemistry and age of the Ontong Java Plateau, in *The Mesozoic Pacific: Geology, Tectonics, and Volcanism, Geophys. Monogr. Ser. 77*, edited by M. S. Pringle, et al., pp. 233–261, AGU, Washington, D. C.
Mahoney, J. J., J. M. Sinton, M. D. Kurz, J. D. Macdougall, K. J. Spencer, and G. W. Lugmair (1994), Isotope and trace element characteristics of a superfast spreading ridge: East Pacific Rise, 13–23°S, *Earth Planet. Sci. Lett.*, *77*, 273–284.
Mahoney, J. J., R. Frei, M. L. G. Tejada, X. X. Mo, P. T. Leat, and T. F. Nägler (1998), Tracing the Indian Ocean mantle domain through time: Isotopic results from old West Indian, East Tethyan, and South Pacific seafloor, *J. Petrol.*, *39*(7), 1285–1306.
Mahoney, J. J., R. A. Duncan, M. L. G. Tejada, W. W. Sager, and T. Bralower (2005), Jurassic-Cretaceous boundary age and mid-ocean-ridge-type mantle source for Shatsky Rise, *Geology*, *33*(3), 185–188.
McCulloch, M. T., R. T. Gregory, G. J. Wasserburg, and H. P. Taylor Jr. (1981), Sm-Nd, Rb-Sr, and $^{18}O/^{16}O$ isotopic systematics in an oceanic crustal section: Evidence from the Samail Ophiolite, *J. Geophys. Res.*, *86*(B4), 2721–2735, doi:10.1029/JB086iB04p02721.
Menard, H. W., S. M. Smith, and T. E. Chase (1964), Guyots in the Southwestern Pacific basin, *Geol. Soc. Am. Bull.*, *75*, 145–148.
Molnar, P. T., T. Atwater, J. Mammerickx, and S. M. Smith (1975), Magnetic anomalies, bathymetry and the tectonic evolution of the South Pacific since the Late Cretaceous, *Geophys. J. R. Astron. Soc.*, *40*, 383–420.
Montelli, R., G. Nolet, F. A. Dahlen, G. Masters, E. R. Engdahl, and S.-H. Hung (2004), Finite-frequency tomography reveals a variety of plumes in the mantle, *Science*, *303*, 338–343.
Mortimer, N., and D. Parkinson (1996), Hikurangi Plateau: A Cretaceous large igneous province in the southwest Pacific Ocean, *J. Geophys. Res.*, *101*(B1), 687–696.
Müller, R. D., M. Sdrolias, C. Gaina, and W. R. Roest (2008), Age, spreading rates, and spreading asymmetry of the world's ocean crust, *Geochem. Geophys. Geosyst.*, *9*, Q04006, doi:10.1029/2007GC001743.
Nakamura, Y., and M. Tatsumoto (1988), Pb, Nd, and Sr isotopic evidence for a multicomponent source for rocks of Cook-Austral islands and heterogeneities of mantle plumes, *Geochim. Cosmochim. Acta*, *52*, 2909–2924.
Neal, C. R., J. J. Mahoney, L. W. Kroenke, R. A. Duncan, and M. G. Petterson (1997), The Ontong Java Plateau, in *Large Igneous Provinces: Continental, Oceanic, and Planetary Flood Volcanism, Geophys. Monogr. Ser. 100*, edited by J. J. Mahoney and M. F. Coffin, pp. 183–216, AGU, Washington, D. C.
Niu, Y.-L., D. G. Waggoner, J. M. Sinton, and J. J. Mahoney (1996), Mantle source heterogeneity and melting processes beneath seafloor spreading centers: East Pacific Rise 18°–19°S, *J. Geophys. Res.*, *101*(B12), 27,711–27,733.
Norrish, K., and B. W. Chappell (1977), X-ray fuorescence spectrometry, in *Physical Methods in Determinative Mineralogy*, 2nd ed., edited by J. Zussman, pp. 201–272, Academic, New York, N. Y.

O'Connor, J. M., B. Steinberger, M. Regelous, A. A. P. Koppers, J. R. Wijbrans, K. M. Haase, P. Stoffers, W. Jokar, and D. Garbe-Schönberg (2013), Constraints on past plate and mantle motion from new ages from the Hawaiian-Emperor Seamount Chain, *Geochem. Geophys. Geosyst.*, *14*, 4564–4584, doi:10.1002/ggge.20267.

Pfänder, J. A., C. Münker, A. Stracke, and K. Mezger (2007), Nb/Ta and Zr/Hf in ocean island basalts—Implications for crust-mantle differentiation and the fate of Niobium, *Earth Planet. Sci. Lett.*, *254*(1–2), 158–172.

Pietruszka, A. P., and M. O. Garcia (1999), A rapid fluctuation in the mantle source and melting history of Kilauea volcano inferred from the geochemistry of its historical summit lavas (1790–1982), *J. Petrol.*, *40*, 1321–1342.

Pilet, S., J. Hernandez, P. Sylverster, and M. Poujol (2005), The metasomatic alternative for ocean island basalt heterogeneity, *Earth Planet. Sci. Lett.*, *236*, 148–166.

Puzankov, Y. M., and V. A. Bobrov (1997), Geochemistry of the volcanic rocks from Easter and Sala y Gomez islands, *Geochem. Int.*, *35*, 609–619.

Ray, J. S., J. J. Mahoney, R. A. Duncan, J. Ray, P. Wessel, and D. F. Naar (2012), Chronology and geochemistry of Lavas from the Nazca Ridge and Easter Seamount Chain: An ~30 Myr hotspot record, *J. Petrol.*, *53*(7), 1417–1448, doi:10.1093/petrology/egs021.

Regelous, M., A. W. Hofmann, W. Abouchami, and S. J. G. Galer (2003), Geochemistry of lavas from the Emperor seamounts, and geochemical evolution of Hawaiian magmatism from 85 to 42 Ma, *J. Petrol.*, *44*, 113–140.

Reiners, P. W., and B. K. Nelson (1998), Temporal-compositional-isotopic trends in rejuvenated-stage magmas of Kauai, Hawaii, and implications for mantle melting processes, *Geochim. Cosmochim. Acta*, *62*, 2347–2368.

Rhodes, J. M., and S. R. Hart (1995), Episodic trace element and isotopic variations in historical Mauna Loa lavas: Implications for magma and plume dynamics, in *Mauna Loa Revealed*, edited by J. M. Rhodes and J. P. Lockwood, pp. 263–288, AGU, Washington, D. C.

Richards, M. A., D. L. Jones, R. A. Duncan, and D. J. DePaolo (1991), A mantle plume initiation model for the formation of Wrangelia and other oceanic flood basalt plateaus, *Science*, *254*, 263–266.

Roden, M. F., F. A. Frey, and D. A. Clague (1984), Geochemistry of tholeiitic and alkalic lavas from the Koolau range, Oahu, Hawaii: Implications for Hawaiian volcanism, *Earth Planet. Sci. Lett.*, *69*, 141–158.

Roden, M. F., T. W. Trull, S. R. Hart, and F. A. Frey (1994), New He, Nd, Pb, and Sr isotopic constraints on the constitution of the Hawaiian plume; results from Koolau volcano, Oahu, Hawaii, USA, *Geochim. Cosmochim. Acta*, *58*, 1431–1440.

Rychert, C. A., and P. M. Shearer (2009), A global view of the lithosphere-asthenosphere boundary, *Science*, *324*(5926), 495–498, doi: 10.1126/science.1169754.

Salters, V. J. M., and A. Stracke (2004), Composition of the depleted mantle, *Geochem. Geophys. Geosyst.*, *5*, Q05004, doi:10.1029/2003GC000597.

Salters, V. J. M., J. Blichert, Z. Fekiacova, A. Sachi-Kocher, and M. Bizimis (2006), Isotope and trace element evidence for depleted lithosphere in the source of enriched Koolau basalts, *Contrib. Mineral. Petrol.*, *151*, 297–312, doi:10.1007/s00410-005-0059-y.

Sclater, J. G., S. Hellinger, and C. Tapscott (1977), The paleobathymerty of the Atlantic from the Jurassic to the present, *J. Geol.*, *5*, 509–552.

Seyfried, W. E., and J. L. Bischoff (1979), Low temperature basalt alteration by seawater: An experimental study at 70°C and 150°C, *Geochim. Cosmochim. Acta*, *43*, 1937–1947.

Shafer, J. T., C. R. Neal, and M. Regelous (2005), Petrogenesis of Hawaiian postshield lavas: Evidence from Nintoku seamount, Emperor seamount chain, *Geochem. Geophys. Geosyst.*, *6*, Q05L09, doi:10.1029/2004GC000875.

Sharp, W. D., and D. A. Clague (2002), An older, slower Hawaii-Emperor bend, *Eos Trans. AGU*, *83*(47), Fall Meet. Suppl., Abstract T61C-04.

Shaw, D. M. (1970), Trace element fractionation during anatexis, *Geochim. Cosmochim. Acta*, *34*, 237–243.

Sheth, H. C., J. J. Mahoney, and A. N. Baxter (2003), Geochemistry of lavas from Mauritius, Indian Ocean: Mantle sources and petrogenesis, *Int. Geol. Rev.*, *45*(9), 780–797.

Sobolev, A., A. W. Hofmann, and I. K. Nikogosian (2000), Recycled oceanic crust observed in 'ghost plagioclase' within the source of Mauna Loa lavas, *Nature*, *404*, 986–990.

Staudigel, H., A. Zindler, S. R. Hart, T. Leslie, C. Y. Chen, and D. Clague (1984), The isotope systematics of a juvenile intraplate volcano: Pb, Nd, and Sr isotope ratios of basalts from Loihi Seamount, Hawaii, *Earth Planet. Sci. Lett.*, *69*, 13–29.

Stearns, H. (1966), *Geology of the State of Hawaii*, 266 pp., Pacific Books, Palo Alto, Calif.

Stein, C. A., and S. Stein (1992), A model for the global variation in oceanic depth and heat flow with lithospheric age, *Nature*, *359*(6391), 123–129.

Stille, P., D. M. Unruh, and M. Tatsumoto (1983), Pb, Sr, Nd, and Hf isotopic evidence of multiple sources for Oahu, Hawaii basalts, *Nature*, *304*, 25–29.

Stoffers, P., et al. (2003), Cruise report Sonne 167: Louisville, *Berichte-Rep. 20*, pp. 276, Christian-Albrechts-Univ. zu Kiel, Inst. für Geowissenschaften, Kiel, Germany.

Stracke, A., and B. Bourdon (2009), The importance of melt extraction for tracing mantle heterogeneity, *Geochim. Cosmochim. Acta*, *73*, 218–238, doi:10.1016/j.gca.2008.10.015.

Stracke, A., A. W. Hofmann, and S. R. Hart (2005), FOZO, HIMU, and the rest of the mantle zoo, *Geochim. Geophys. Geosyst.*, *6*, Q05007, doi: 10.1029/2004GC000824.

Tarduno, J. A., W. V. Sliter, L. Kroenke, M. Leckie, H. Mayer, J. J. Mahoney, R. Musgrave, M. Storey, and E. L. Winterer (1991), Rapid formation of Ontong Java Plateau by Aptian mantle plume volcanism, *Science*, *254*, 399–403.

Tatsumoto, M. (1988), U, Th and Pb abundances in Hawaiian xenoliths, paper presented at Conference on Origin of the Earth, pp. 89–90, Lunar Planet. Inst., Houston, Tex.

Taylor, B. (2006), The single largest oceanic plateau: Ontong Java–Manihiki–Hikurangi, *Earth Planet. Sci. Lett.*, *241*, 372–380.

Tegner, C., C. L. Lesher, L. M. Larsen, and W. S. Watt (1998), Evidence from the rare-earth-element record of mantle melting for cooling of the Tertiary Iceland plume, *Nature*, *395*, 591–594.

Tejada, M. L. G., J. J. Mahoney, R. A. Duncan, and M. P. Hawkins (1996), Age and geochemistry of basement and alkalic rocks of Malaita and Santa Isabel, Solomon Islands, southern margin of Ontong Java Plateau, *J. Petrol.*, *37*, 361–394.

Tejada, M. L. G., J. J. Mahoney, C. R. Neal, R. A. Duncan, and M. G. Petterson (2002), Basement geochemistry and geochronology of central Malaita, Solomon Islands, with implications for the origin and evolution of the Ontong Java Plateau, *J. Petrol.*, *43*, 449–484.

Tejada, M. L. G., J. J. Mahoney, P. R. Castillo, S. P. Ingle, H. C. Sheth, and D. Weis (2004), Pin-pricking the elephant: Evidence on the origin of the Ontong Java Plateau from Pb-Sr-Hf-Nd isotopic characteristics of ODP Leg 192 basalts, in *Origin and Evolution of the Ontong Java Plateau, Spec. Publ. 229*, edited by J. G. Fitton et al., pp. 133–150, Geol. Soc. of London, London, U. K.

Timm, C., K. Hoernle, R. Werner, F. Hauff, P. van den Bogaard, P. Michael, M. F. Coffin, and A. Koppers (2011), Age and geochemistry of the oceanic Manihiki Plateau, SW Pacific: New evidence for a plume origin, *Earth Planet. Sci. Lett.*, *304*, 135–146, doi:10.1016/j.epsl.2011.01.025.

Timm, C., D. Bassett, I. J. Graham, M. I. Leybourne, C. E. J. de Ronde, J. Woodhead, D. Layton-Matthews, and A. B. Watts (2013), Louisville seamount subduction and its implication on mantle flow beneath the central Tonga-Kermadec arc, *Nat. Commun.*, *4*, 1720, doi:10.1038/ncomms2702.

Turcotte, D. L., and G. Schubert (1982), *Geodynamics: Applications of Continuum Physics to Geological Problems*, 450 pp., John Wiley, New York.

Verma, S. P. (1992), Seawater alteration effects on REE, K, Rb, Cs, Sr, U, Th, Pb and Sr-Nd-Pb isotope systematics of Mid-Ocean Ridge Basalt, *Geochem. J.*, *26*, 159–177.

Waggoner, D. G. (1993), The age and alteration of central Pacific oceanic crust near Hawaii, site 843, in *Proceedings of Ocean Drilling Program Initial Report*, vol. 136, edited by R. H. Wilkens et al., pp. 119–132, Ocean Drill. Program, College Station, Tex.

Watts, A. B., J. K. Weissel, R. A. Duncan, and R. L. Larson (1988), Origin of the Louisville ridge and its relationship to the Eltanin fracture zone system, *J. Geophys. Res.*, *93*(B4), 3051–3077.

Weaver, B. L. (1991), The origin of ocean island end-member compositions: Trace element and isotopic constraints, *Earth Planet. Sci. Lett.*, *104*, 381–397.

Weis, D., M. O. Garcia, J. M. Rhodes, M. Jellinek, and J. S. Scoates (2011), Role of the deep mantle in generating the compositional asymmetry of the Hawaiian mantle plume, *Nat. Geosci.*, *4*, 831–838, doi:10.1038/ngeo1328.

Wessel, P., and L. W. Kroenke (2008), Pacific absolute plate motion since 145 Ma: An assessment of the fixed hot spot hypothesis, *J. Geophys. Res.*, *113*, B06101, doi:10.1029/2007JB005499.

Wessel, P., and L. W. Kroenke (2009), Observations of geometry and ages constrain relative motion of Hawaii and Louisville plumes, *Earth Planet. Sci. Lett.*, *284*, 467–472.

Wessel, P., and W. H. F. Smith (1991), Free software helps map and display data, *Eos Trans. AGU*, *72*(441), 445–446.

Wessel, P., and W. H. F. Smith (1998), New, improved version of the generic mapping tools released, *Eos Trans. AGU*, *79*, 579.

West, H. B., and W. P. Leeman (1987), Isotopic evolution of lavas from Haleakala crater, Hawaii, *Earth Planet. Sci. Lett.*, *84*, 211–225.

West, H. B., D. C. Gerlach, W. P. Leeman, and M. O. Garcia (1987), Isotopic constraints on the origin of Hawaiian lavas from the Maui volcanic complex, Hawaii, *Nature*, *330*, 216–220.

White, W. M., and R. A. Duncan (1996), Geochemistry and geochronology of the Society islands: New evidence for deep mantle recycling, in *Earth Processes, Reading the Isotopic Code*, edited by A. Basu and S. R. Hart, pp. 183–206, AGU, Washington D. C.

Woodhead, J. D., and M. T. McCulloch (1989), Ancient seafloor signals in Pitcairn Island lavas and evidence for large amplitude, small length-scale mantle heterogeneities, *Earth Planet. Sci Lett.*, *94*, 257–273.

Worthington, T. J., R. Hekinian, P. Stoffers, Th. Kuhn, and F. Hauff (2006), Osbourn Trough: Structure, geochemistry and implications of a mid-Cretaceous paleospreading ridge in the South Pacific, *Earth Planet. Sci. Lett.*, *245*, 685–701.

Zindler, A., and S. Hart (1986), Chemical geodynamics, *Ann. Rev. Earth Planet. Sci.*, *14*, 493–571.